Geochimica et Cosmochimica Acta 408 (2025) 12–27

Contents lists available at ScienceDirect

Geochimica et Cosmochimica Acta

journal homepage: www.elsevier.com/locate/gca

Using carbon isotopes to trace the origin of volatiles on Earth and Mars

Damanveer S. Grewal [a,*], Sujoy Mukhopadhyay [b]

[a] Department of Earth and Planetary Sciences, Yale University, New Haven, CT 06511, USA
[b] School of Earth and Space Exploration, Arizona State University, Tempe, AZ 85281, USA

ARTICLE INFO

Associate editor: Yves Marrocchi

Keywords:
Carbon
Earth
Mars
Meteorites
Chondrites
Origin of volatiles

ABSTRACT

The distinct accretionary histories of Earth and Mars – with Earth experiencing protracted growth and small contributions from outer solar system (carbonaceous, CC) materials, and Mars undergoing rapid growth with building materials drawn almost exclusively from the inner solar system (non-carbonaceous, NC) – highlight key differences in planetary formation. These contrasts underscore the importance of a comparative planetology framework for understanding the origin of volatiles in terrestrial planets. In this study, we examined the relationship between the carbon (C) isotopic compositions of planetary and planetesimal reservoirs to trace the origin of volatiles on Earth and Mars. The mean δ^{13}C value of magmatic C in Martian meteorites (−20 ‰) is significantly lower than that of the bulk silicate Earth (BSE), with a canonical value of −5 ‰. While basaltic achondrites, magmatic iron meteorites, and ordinary chondrites from the NC reservoir display δ^{13}C values similar to Martian meteorites, the BSE δ^{13}C value is comparable to volatile-rich CC chondrites such as CI, CM, and CR, as well as with enstatite chondrites and ureilites from the NC reservoir. If Martian magmas underwent minimal C isotopic fractionation during degassing or degassed under kinetic conditions, then the δ^{13}C value of the Martian mantle likely reflects accretion from thermally processed undifferentiated (ordinary chondrite-like) and differentiated NC materials. In contrast, if extensive degassing occurred via Rayleigh fractionation under equilibrium conditions, the δ^{13}C value of the Martian mantle would have a higher δ^{13}C value (−12 to −10 ‰) than that recorded in Martian meteorites – though still lighter than that of the canonical BSE δ^{13}C. This implies a contribution from relatively ^{13}C-rich NC materials, potentially similar to enstatite chondrites. For BSE, although the canonical δ^{13}C value of –5 ‰ overlaps with those of enstatite chondrites and ureilites, the late-stage delivery of volatile-rich CC materials during the main phase of Earth's growth, which was critical for establishing its water and nitrogen inventories, likely biased its C isotopic composition towards a CC-like signature. However, a lower mean δ^{13}C value of −8.4 ‰ of the MORB mantle, as proposed by recent studies, could mean that Earth's mantle still preserves the primordial signature of ^{13}C-poor, thermally processed NC materials accreted during the early stages of the planet's growth. The observed heterogeneity in mantle C isotopic compositions, similar to that seen in H and N isotopes, could therefore reflect a mixed contribution from both NC and CC materials. Thus, the δ^{13}C value of the BSE could be lower than the canonical estimate and may align more closely with the proposed value for the MORB mantle. Taken together, these findings suggest that the contrasting accretionary histories of Earth and Mars led to fundamentally different pathways for volatile acquisition. These divergent pathways likely shaped the long-term geochemical evolution of each planet and influenced their potential for habitability.

1. Introduction

Understanding the origins of highly volatile elements such as carbon (C), nitrogen (N), and hydrogen (H) on Earth and Mars is crucial for deciphering the early solar system processes that shaped the volatile inventories of terrestrial planets (Marty, 2012; Halliday, 2013; Hirschmann, 2016; Dasgupta and Grewal, 2019). These two planets have distinct growth histories: Earth experienced protracted accretion over tens of Myrs, whereas Mars underwent rapid growth within a few Myrs of the solar system's formation (Kleine et al., 2009; Dauphas and Pourmand, 2011). Nucleosynthetic anomalies in several non-volatile elements indicate that Mars accreted almost entirely from materials sourced from the inner solar system (non-carbonaceous (NC) reservoir), whereas Earth accreted a significant proportion of its mass (~5%) from materials originating in the outer solar system (carbonaceous (CC) reservoir) (Dauphas, 2017; Burkhardt et al., 2021; Dauphas et al., 2024;

---

* Corresponding author.
E-mail address: damanveer.grewal@yale.edu (D.S. Grewal).

https://doi.org/10.1016/j.gca.2025.09.014
Received 22 May 2025; Accepted 9 September 2025

Nimmo et al., 2024). Thus, investigating the origins of C–N–H on Earth and Mars from a comparative planetology perspective can provide valuable insights into the distribution of volatile reservoirs in the solar protoplanetary disk and the role of early solar system dynamics in shaping the volatile inventories of terrestrial planets.

The lack of a third stable isotope for C–N–H limits the ability to correct for mass-dependent isotope fractionation after accretion, which is important for determining the isotopic compositions of primordial materials. Despite this limitation, comparisons of C–N–H isotopic ratios between cosmochemical and terrestrial reservoirs have provided important insights. The large variations in N and H isotopes among cosmochemical reservoirs (e.g., comets, meteorites, and the solar nebula) make them the preferred tool for this analysis (Marty, 2012; Alexander et al., 2012; Halliday, 2013). Due to the inaccessibility of planetary cores, our understanding of the origin of C–N–H on Earth and Mars is entirely based on the bulk silicate reservoirs of these planets (BSE for Earth and BSM for Mars). The general overlap of N and H isotopic compositions in the BSE and Martian meteorites with different groups of meteorites suggests that the C–N–H inventories of terrestrial planets were predominantly derived from early solar system rocky bodies, with minimal contributions from nebular or cometary sources (Mathew and Marti, 2001; Mathew et al., 2003; Mohapatra and Murty, 2003; Marty, 2012; Alexander et al., 2012; Usui et al., 2012; Halliday, 2013; Peslier et al., 2019). Since the BSE is depleted in C–N–H by ∼ 2–3 orders of magnitude compared to volatile-rich CI and CM chondrites (Marty, 2012; Halliday, 2013), even a small contribution from such chondritic materials during the later stages of Earth's growth could explain the present-day C–N–H inventory in the BSE. Accretion of such volatile-rich materials during the later stages is preferred because Earth's accretion likely involved several energetic collisions, which likely caused multiple episodes of core formation and atmospheric loss (Rubie et al., 2011; Tucker and Mukhopadhyay, 2014; Schlichting and Mukhopadhyay, 2018; Sakuraba et al., 2021). The siderophile and atmophile behavior of C–N–H (Dasgupta et al., 2013; Dalou et al., 2017; Grewal et al., 2019b, a, 2021b, a; Hakim et al., 2019; Tagawa et al., 2021; Li et al., 2023; Suer et al., 2023), combined with Ag, Mo, and Zn isotope systematics (Schönbächler et al., 2010; Budde et al., 2019; Nimmo et al., 2024), supports the hypothesis that the C–N–H inventory in the BSE is skewed toward contributions from the later stages of Earth's formation (Marty, 2012; Grewal et al., 2019b, 2021b, 2024a; Alexander, 2022; Tsuno et al., 2024; Grewal and Manilal, 2025). While it is generally argued that the C–N–H inventory in the BSE primarily originated from a CC chondrite-like materials (Marty, 2012; Alexander et al., 2012; Halliday, 2013), the resemblance in N and H isotopic compositions between several NC chondrites, achondrites, and certain samples from Earth's mantle suggests that inner solar system materials, which contributed ∼ 95 % of Earth's mass, may have played an important role in shaping the BSE's C–N–H inventory (Javoy, 1995; Piani et al., 2020; Grewal et al., 2021c, 2025a). Although the C–N–H inventory in the BSM is less well-characterized, scarce data from Martian meteorites suggest that the BSM is even more depleted in C–N–H than the BSE (McCubbin et al., 2012; Tsuno et al., 2018; Yoshizaki and McDonough, 2020). However, the limited contribution of CC materials, combined with Mars' rapid growth, likely resulted in its accretion from thermally processed materials. In contrast, Earth, which may have acquired a significant portion of its CC material inventory from more primitive sources, points towards fundamental differences in the origins of C–N–H on Earth and Mars.

Recent findings based on nucleosynthetic anomalies in Zn, a moderately volatile element (MVE), provide valuable insights into the differences in the origins of C–N–H on Earth and Mars. This is because both MVEs and C–N–H are concentrated in the CI-like matrix component of primordial materials sampled by chondrites (Albarède et al., 2013; Alexander et al., 2018b). For instance, C and Zn are correlated across NC and CC chondrites, except for the anomalously reduced enstatite chondrites which likely formed under distinct nebular conditions (Fig. 1).

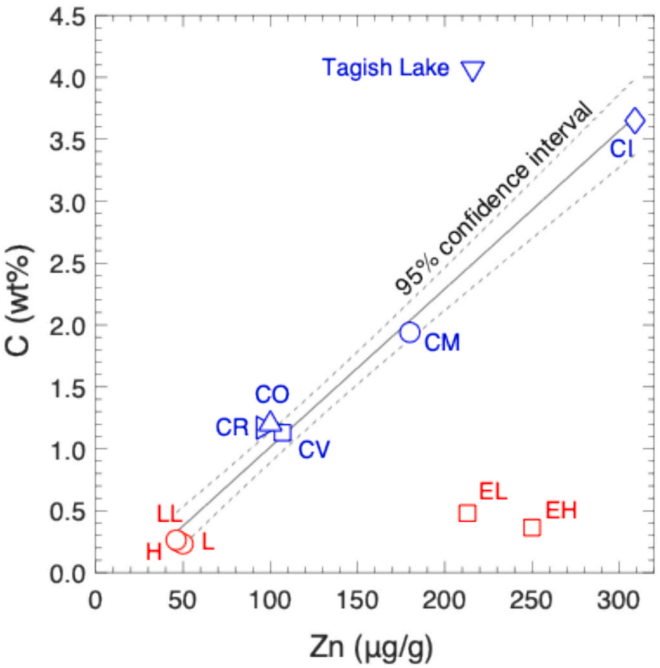

Fig. 1. Carbon versus zinc abundances in meteorites. The plot shows a broad correlation between C and Zn concentrations across various chondrite groups, including CI, CM, CR, CV, CO, and ordinary chondrites (H, L, LL), suggesting that these elements co-occur in similar carrier phases. Notable outliers include the enstatite chondrites (EH, EL), which are extremely reduced, and the Tagish Lake chondrite, which has experienced significant aqueous alteration and is anomalously enriched in carbonates. The dashed lines represents the 95% confidence interval for the linear regression.

Studies indicate that ∼30 % of Zn in the BSE is derived from the CC reservoir, with the remainder originated from the NC reservoir (Steller et al., 2022; Savage et al., 2022; Martins et al., 2023). Assuming a CI chondrite-like Zn concentration as representative of CC materials corresponds to a CC mass fraction of ∼0.05 for Earth, which aligns closely with the ∼5 % contribution of CC-derived materials inferred from nucleosynthetic anomalies in non-volatile elements (Steller et al., 2022). Accretion of this mass of CI-like materials can deliver more than the present-day C–N–H inventory in the BSE. However, the relative contributions of NC and CC materials to the C–N–H inventory in the BSE cannot be determined with the same level of precision as Zn. This uncertainty arises from the limited understanding of the bulk N and H isotopic compositions of Earth's mantle, which is influenced by large variations in N and H isotopic compositions within the different mantle reservoirs and the lack of constraints on the relative N and H inventories of these reservoirs (Deloule et al., 1991; Cartigny and Marty, 2013; Loewen et al., 2019). Furthermore, the substantial overlap in N and H isotopic compositions between NC and CC chondrites complicates efforts to disentangle the contributions of these reservoirs to Earth's volatile budget. For instance, the N isotopic compositions of Earth's mantle overlaps with the negative δ^{15}N values observed in CV and CO chondrites, and NC chondrites and iron meteorites (Grewal et al., 2021c; Grewal, 2022; Broadley et al., 2022). Similarly, the H isotopic compositions of CM, CO, and CV overlap with negative δD values observed in NC chondrites and Earth's mantle (Piani et al., 2020). For Mars, isotopic data for Zn indicates that nearly its entire volatile inventory originated from the NC reservoir (Paquet et al., 2023; Kleine et al., 2023). This finding is consistent with nucleosynthetic anomalies in non-volatile elements, which also suggest minimal contributions from CC materials to Mars (Burkhardt et al., 2021; Dauphas et al., 2024). However, the overlap in isotopic composition of H (Usui et al., 2012; Peslier et al., 2019) and N (Mohapatra and Murty, 2003; Deligny et al., 2023) between

Martian meteorites and carbonaceous chondrites, which may be due to larger uncertainties in the former, poses a challenging problem given the near-complete absence of CC-derived materials in Mars' accretion.

In this study, we examine the C isotopic compositions of planetary and planetesimal reservoirs, leveraging recent advances in understanding of the provenance of NC and CC materials in planetary formation, to shed new light on the origin of C–N–H on Earth and Mars. Carbon isotopic compositions have been relatively underutilized in these investigations because, unlike N and H isotopes, the C isotopic variations in cosmochemical reservoirs are less pronounced. However, using C isotopes as a proxy provides an important advantage over N and H isotopes in determining the origin of C–N–H in terrestrial planets. Unlike N and H isotopic compositions, C isotopic ratios in the BSE and Martian meteorites show limited variations. This allows the C isotopic compositions of the BSE and BSM to be better constrained, enabling a clearer determination of the contributions from NC and CC materials to their C–N–H inventories.

2. Carbon isotopic composition of BSE and Martian meteorites

Recent estimates suggest that up to 90 % of the C inventory in the BSE may be stored in the mantle (Marty, 2012; Marty et al., 2020); however, significantly lower estimates have also been proposed (Halliday, 2013; Hirschmann, 2018). The most reliable estimate for the $\delta^{13}C$ value of Earth's MORB mantle (−5‰) comes from the C isotopic composition of CO_2 gas trapped in vesicles within "popping rocks", which are thought to have undergone no degassing (Javoy and Pineau, 1991; Pineau et al., 2004). Peridotitic diamonds also suggest a broadly similar $\delta^{13}C$ value for the upper mantle (−5‰) (Cartigny et al., 1998; Cartigny, 2005). Occasionally, lower $\delta^{13}C$ values have been observed in MORB glasses, volcanic gases, and diamonds (Cartigny et al., 1998; Deines, 2002; Marty et al., 2013; Aubaud, 2022). In the case of MORB glasses and volcanic gases, these lighter C isotopic signatures are attributed to equilibrium isotopic fractionation during degassing and/or the incorporation of subducted C in the mantle source that is preferentially enriched in organic over inorganic material (Mattey, 1991; Aubaud, 2022; Lee et al., 2024). For diamonds, the lower $\delta^{13}C$ values are thought to result from the incorporation of recycled organic C and/or isotopic fractionation during diamond formation (Cartigny et al., 1998; Deines, 2002; Cartigny, 2005). Earth's surface C, primarily composed of carbonates ($\delta^{13}C \sim 0$ ‰) and biogenic organics ($\delta^{13}C \sim -25$ ‰) in a ~4:1 ratio, exhibits a bulk $\delta^{13}C$ value close to −5 ‰ (Deines, 2002). This value is strikingly similar to the canonical $\delta^{13}C$ of the upper mantle, which appears to have remained relatively constant throughout geological history (Deines, 2002).

However, recent studies based on the *in-situ* C isotope measurements in CO_2 undersaturated basalt glasses and melt inclusions, using secondary ion mass spectrometry (SIMS), have challenged the notion that a $\delta^{13}C$ value of −5 ‰ is representative of the MORB mantle (Moussallam et al., 2025a, b; Moussallam, 2025). These studies showed that while samples from Atlantic display $\delta^{13}C$ values similar to the canonical MORB mantle, those from the Arctic, Indian, and Pacific basins display lower values, with a mean of −8.4 ‰. The authors suggested that this lower mean value may better represent the global upper mantle $\delta^{13}C$ signature outside the Atlantic, whereas the −5 ‰ value preserved in peridotitic diamonds may reflect only subcratonic mantle domains. If correct, this would require a revision of the BSE $\delta^{13}C$ estimate to lower values (Moussallam et al., 2025b). Regardless of whether −5 ‰ or lower $\delta^{13}C$ values better represent the C isotopic composition of the MORB mantle, and as an extension the BSE – a question future work should address – the relatively narrow range of mean $\delta^{13}C$ values in the BSE contrasts with the wide variability observed in the mantle's N and H isotopic compositions. This narrow $\delta^{13}C$ range provides a comparatively stringent constraint for tracing the origin of C in the BSE (Fig. 2).

Estimating the C isotopic composition of the BSM is significantly more challenging than for the BSE due to the scarcity of Martian rock samples. While carbonates are present on the Martian surface, their contribution to the mantle's C budget is likely minimal (Wright et al., 1992; Jull et al., 1995). This is because Mars lacked Earth-style plate tectonics (Sleep, 1994; Breuer and Spohn, 2003), resulting in limited or no cycling of C between surface and interior reservoirs (Wright et al., 1990; Grady et al., 2004). Previous studies have focused on meteorites

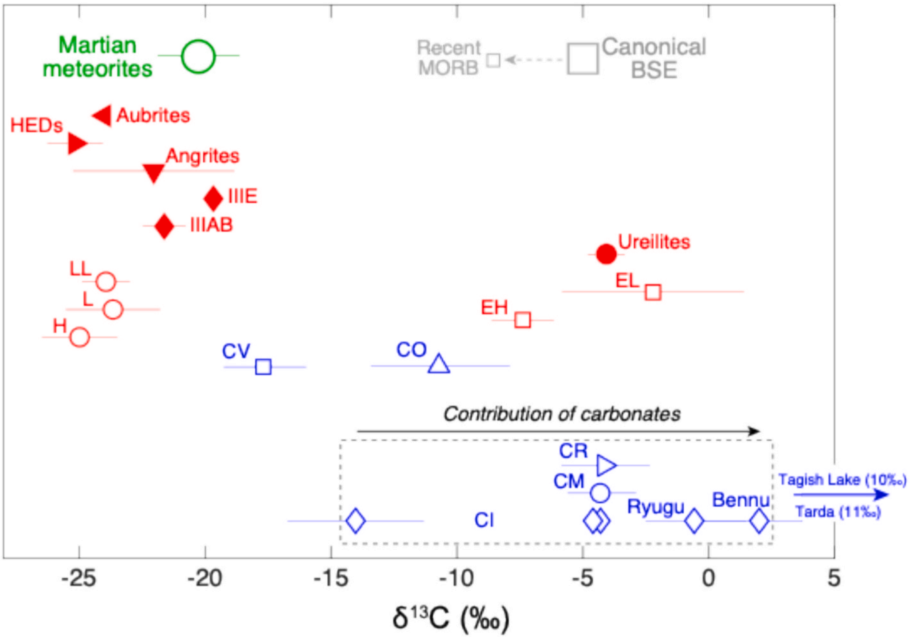

Fig. 2. Bulk $\delta^{13}C$ values of carbonaceous chondrites, ordinary chondrites, enstatite chondrites, ureilites, differentiated achondrites (angrites, HEDs, aubrites), and magmatic iron meteorites (IIIAB, IIIE), compared to Martian meteorites and the canonical BSE estimate. The newly determined mean value of the MORB mantle is also plotted for comparison. Carbonaceous chondrites exhibit the widest $\delta^{13}C$ range, with elevated values largely attributed to the contribution of ^{13}C-rich carbonates. Ordinary chondrites and differentiated meteorites, including Martian meteorites, generally show more ^{13}C-depleted values. Data and references are reported in Table 1 and Supplementary Table 1.

such as Chassigny (dunite) and shergottites (mafic to ultramafic partial melts) to constrain the primary magmatic C isotopic signature of the Martian mantle (Carr et al., 1985; Wright et al., 1990; Grady et al., 1997a, 2004; Steele et al., 2012). These meteorites are preferred because they lack secondary carbonates formed through surface aqueous processes. Abundance and isotope data of magmatic C in Martian meteorites have been reported for acid-washed samples (to remove carbonates from both Martian sources and terrestrial weathering) using stepped combustion mass spectrometry between 600 °C (below which terrestrial organic contamination is prevalent) and 1000 °C (above which trapped Martian atmospheric CO_2 is released) (Wright et al., 1990; Grady et al., 1997a, 2004). The $\delta^{13}C$ values for all shergottites, including Zagami and Tissint (witnessed falls), consistently vary between −24 and −16 ‰, irrespective of age or petrogenetic origin (Grady et al., 1997a, 2004; Steele et al., 2012). Chassigny (a dunite and also a fall) exhibits a $\delta^{13}C$ value of −21 ‰ (Grady et al., 2004), i.e., within the range of shergottites. Despite relatively large variations in C abundances (~1–100 μg/g) across Martian meteorites, no correlation exists between C abundance and $\delta^{13}C$ values (Grady et al., 2004). Collectively, Martian meteorites exhibit a mean $\delta^{13}C$ value of −20 ± 3 ‰ (95 % c.i.) (Fig. 2, Table 1). This value is within the same range as buried and metamorphosed organic C in terrestrial rocks. Although abiotic macromolecular C (amorphous to poorly ordered graphite) is ubiquitous in Martian meteorites, the association of organic C within magmatic minerals suggests that reduced C precipitated during magma crystallization and does not represent buried and metamorphosed organic C (Steele et al., 2012). Thus, unlike Earth's mantle xenoliths, the mean $\delta^{13}C$ value of −20 ‰ in Martian meteorites originates from C in the Martian mantle, rather than from subducted organic C.

Table 1
Carbon abundances and isotopic compositions of planetesimal and planetary reservoirs.

Sample	Mean C (μg/g)	Max C (μg/g)	Min C (μg/g)	$\delta^{13}C$ (‰)	95 % ci
EH[1]	1914	2371	270	−7.4	1.2
EL[1]	3205	5094	1617	−2.2	3.6
H[2]	2538	17,770	100	−25.0	1.5
L[2]	2314	9200	500	−23.7	1.9
LL[2]	2630	9500	300	−23.9	1.0
Tagish Lake[3]	37,173	42,500	21,400	10.2	3.2
Tarda[4]	40,567	41,100	40,000	10.9	0.4
CM[3]	23,717	40,500	400	−4.3	1.4
CR[3]	12,989	27,400	10,022	−4.2	1.8
CV[3]	7286	15,000	750	−17.7	1.6
CO[3,5]	6945	12,046	926	−10.7	2.8
CI-Orgueil[3]	37,200	–	–	−14.0	2.7
CI-Ivuna[3]	35,000	–	–	−4.3	–
CI-Alais[3]	54,000	–	–	−4.6	–
Bennu[6]	45,667	47,000	45,000	2.0	2.5
Ryugu[7]	46,300	48,600	44,000	−0.6	2.0
Ureilites[8]	14,920	20,600	10,700	−4.1	0.7
IIIAB[9]	–	–	–	−21.6	0.9
IIIE[9]	–	–	–	−19.7	–
Angrites (plutonic)[10]	48	138	2	−22.0	3.2
HEDs[11]	14	27	2	−25.2	1.1
Aubrites[12]	250	–	–	−24.0	–
Martian meteorites[13]	19	109	1	−20.3	1.6
BSE-canonical[14]	–	450	140	−5.0	–
MORB-recent[15]	–	–	–	−8.4	–

Note: Refer to Table S2 for details of the temperature steps used to estimating the $\delta^{13}C$ values of various meteorite groups.

References: (1) – (Grady et al., 1986); (2) – (Grady et al., 1982, 1989; Vacher et al., 2020); (3) – (Pearson et al., 2006; Alexander et al., 2012; Vacher et al., 2020); (4) – (Marrocchi et al., 2021); (5) – (Alexander et al., 2018a); (6) – (Lauretta et al., 2024); (7) – (Naraoka et al., 2023; Yokoyama et al., 2023); (8) – (Grady et al., 1985; Russell et al., 1993; Smith et al., 2001; Downes et al., 2015; Barrat et al., 2017); (9) – (Deines and Wickman, 1975); (10) – (Abernethy et al., 2013, 2018); (11) – (Grady et al., 1997b; Abernethy et al., 2018); (12) – (Grady et al., 1986); (13) – (Grady et al., 2004; Steele et al., 2012); (14) – (Deines, 2002); (15) – (Moussallam et al., 2025b).

3. Carbon isotopic compositions of chondrites and achondrites

To place the C isotopic composition of the BSE and Martian meteorites into the context of early solar system objects, it is necessary to examine variations in the isotopic signatures of chondrites and achondrites from the NC and CC reservoirs. We focus on carbonaceous chondrites (CI, CM, CO, CV, and CR), ordinary chondrites (H, L, and LL), enstatite chondrites (EH and EL), primitive achondrites (ureilites), mafic achondrites (angrites, HEDs, and aubrites), and magmatic iron meteorites (IIIAB and IIIE groups). These meteorites, whose isotopic characteristics are well studied, represent a diverse sampling of planetesimal reservoirs that have experienced varying degrees of parent body processing. We acknowledge that the factors influencing these signatures are likely more complex than the somewhat simplified discussion presented in this section. Nevertheless, even first-order interpretations can provide valuable insights into variations among early solar system objects and their potential contributions to the C inventories of terrestrial planets. These interpretations, despite their limitations, serve as a crucial starting point for understanding the origin of C in terrestrial planets. Data compilation is reported in Table 1 and Table S1, and the methodology used to collect the data is reported in Table S2.

3.1. Carbonaceous chondrites

Carbon in the carbonaceous chondrites is found in the CI chondrite-like matrix (Alexander et al., 2012; Alexander et al., 2018b). In the matrix, carbonaceous organics serve as the primary C carrier (Alexander et al., 1998, 2017; Glavin et al., 2018), but aqueously altered chondrites often also contain ^{13}C-rich secondary carbonates (Alexander et al., 2015). A relatively uniform ratio of interstellar nanodiamonds to organic material suggests that all carbonaceous chondrites likely accreted a common organic precursor (Alexander et al., 1998). The organic matter in chondrites can be broadly categorized into soluble organic matter (SOM), which comprises a complex mixture of compounds such as amino acids and aliphatic and aromatic hydrocarbons, and insoluble organic matter (IOM), a macromolecular material rich in polycyclic aromatic hydrocarbons (PAHs) (Alexander et al., 1998, 2017; Sephton et al., 2000; Glavin et al., 2018). Even in the most primitive meteorites, SOM concentrations rarely exceed a few hundred parts per million (Gilmour, 2003). This is likely caused by the loss of labile, ^{13}C-rich SOM during low-temperature aqueous alteration (Sephton et al., 2003; Foustoukos et al., 2021). However, this may also partly represent analytical limitations as no reliable method currently exists for the complete extraction of SOM The bulk of the organic component in carbonaceous chondrites is therefore typically assumed to be made up of IOM, which has $\delta^{13}C$ values between − 25 and −5 ‰ (Sephton et al., 2003; Alexander et al., 2007).

The bulk $\delta^{13}C$ values of the three CI chondrites–Orgueil, Alais, and Ivuna–range from−14 to−4 ‰ (Fig. 2, Table 1) (Pearson et al., 2006; Alexander et al., 2012; Vacher et al., 2020). Samples from CI-like asteroids, such as Ryugu and Bennu, exhibit slightly higher $\delta^{13}C$ values (−1‰ and 2 ‰, respectively) (Naraoka et al., 2023; Yokoyama et al., 2023; Lauretta et al., 2024). Tagish Lake and Tarda, type C2 ungrouped carbonaceous chondrites, display distinctly higher $\delta^{13}C$ value of ~ 10–11 ‰ (Pearson et al., 2006; Alexander et al., 2012; Vacher et al., 2020; Marrocchi et al., 2021). Unheated CM and CR chondrites exhibit $\delta^{13}C$ values within a similar range (−4 ± 1 ‰ and−4 ± 2 ‰, respectively) (Fig. 2, Table 1) (Pearson et al., 2006; Alexander et al., 2012). Variations in $\delta^{13}C$ values amongst these chondrites are primarily controlled by the proportion of bulk C present as carbonates, which exhibit significantly higher $\delta^{13}C$ values (60–80 ‰) compared to the C in the organic component (Fig. 3) (Alexander et al., 2015). For instance,

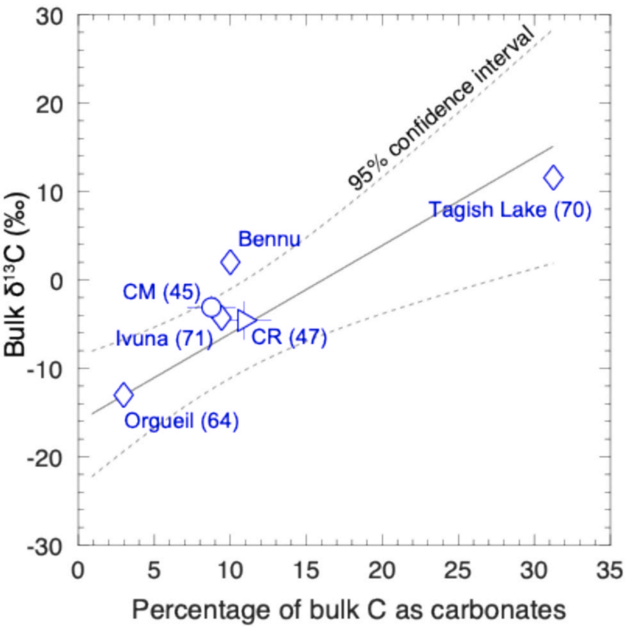

Fig. 3. Relationship between bulk δ^{13}C values and the proportion of bulk C present as carbonates in carbonaceous chondrites. The data illustrate that higher bulk δ^{13}C values are correlated with increased carbonate content, indicating that ^{13}C-enriched carbonates play a significant role in controlling the bulk C isotopic composition of these meteorites. Bracketed values represent the mean δ^{13}C value of the carbonate component. The dashed lines indicates the 95% confidence interval of the linear regression. Data: Percentage of bulk C as carbonates – (Alexander et al., 2015; Lauretta et al., 2024); Bulk δ^{13}C values and the relevant references are reported in Table 1.

Tagish Lake, with ~ 32 % of its bulk C in the form of carbonates, has a significantly higher bulk δ^{13}C value than Orgueil, which contains only ~ 3 % of its C as carbonates. The ^{13}C-rich nature of carbonates has been attributed to alteration by fluids derived from accreted ^{13}C-rich CO_2-CO-rich ices similar to those found in comets (Fujiya et al., 2019, 2023). In contrast, thermally metamorphosed CO and CV chondrites, which lack the carbonate component, display distinctly lower bulk δ^{13}C values (−11 ± 3 ‰ and−18 ± 2 ‰, respectively) compared to other volatile-rich carbonaceous chondrites (Fig. 2, Table 1) (Pearson et al., 2006; Alexander et al., 2012).

3.2. *Ordinary chondrites*

Ordinary chondrites are classified into three groups (H, L, and LL) based on variations in Fe content and are thought to originate from at least three distinct parent bodies (Wasson, 1972). Carbon in ordinary chondrites is primarily found in C-rich aggregates, which consist of fine-scale intergrowths of poorly graphitized and amorphous carbon, with minor contributions from organic species, carbides, elemental carbon dissolved in metal, and graphite (Grady et al., 1982, 1989; Scott et al., 1987). The C-rich aggregates were likely the result of thermal processing that catalyzed the graphitization of carbonaceous material (Scott et al., 1987; Grady et al., 1989). The similarity in the ratios of interstellar nanodiamonds to organic carbon between ordinary and carbonaceous chondrites suggests a common organic precursor (Alexander et al., 1998). Since most ordinary chondrites classified as “finds” are affected by terrestrial contamination or weathering, “falls” have been preferred to track the bulk C and its compositions in H, L, and LL parent bodies (Grady et al., 1982, 1989). Carbon content decreases with the degree of thermal metamorphism, as indicated by petrological type, in unequilibrated ordinary chondrites (type 3) but does not decrease further in equilibrated ordinary chondrites with increasing metamorphic grade (types 4–6) (Fig. 4**A**). The C isotopic compositions of equilibrated ordinary chondrites are relatively ^{13}C-poor and exhibit less variability compared to the ^{13}C-rich compositions observed in unequilibrated ordinary chondrites (Fig. 4**B**). No straightforward correlation exists between bulk C content and its isotopic composition (Grady et al., 1989). Combining the data across all petrologic types, the bulk δ^{13}C values for H (−25 ± 2 ‰), L (−24 ± 2 ‰), and LL (−24 ± 2 ‰) are remarkably consistent and significantly lower than those of the ^{13}C-rich carbonaceous chondrites (Fig. 2, Table 1).

3.3. *Enstatite chondrites*

Carbon in the highly reduced enstatite chondrites, which are

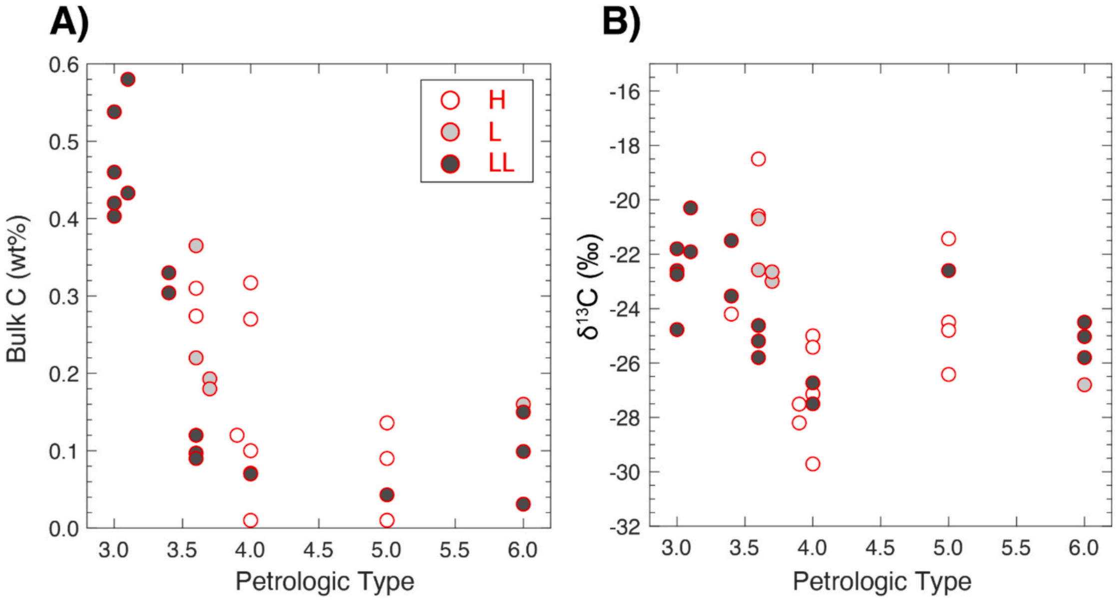

Fig. 4. (**A**) Carbon abundances and (**B**) bulk δ^{13}C values of ordinary chondrites plotted as a function of petrologic type. (**A**) Carbon abundance decreases with increasing thermal metamorphism from type 3 to type 4, but shows no significant decline beyond type 4. (**B**) Bulk δ^{13}C values of equilibrated ordinary chondrites (types 4–6) are exhibit limited variability, in contrast to the more variable δ^{13}C values observed in unequilibrated type 3 chondrites. Data and references are reported in Supplementary Table 1.

subdivided into EH and EL groups based on Fe content, is predominantly present as graphite, with minor contributions from cohenite as an accessory phase and organics (Grady et al., 1986; Storz et al., 2021). Enstatite chondrites are unique among chondrites in that thermal processing did not lead to a decrease in their C content (Grady et al., 1986). This phenomenon is likely linked to their highly reduced nature, where C, present in refractory forms like graphite, was able to withstand devolatilization. Graphite in enstatite chondrites typically occurs in two characteristic assemblages: silicate-associated graphite (SAG) and metal-associated graphite (MAG) (Storz et al., 2021). MAG graphite is commonly attributed to C exsolution from taenite during cooling. The majority of the C in enstatite chondrites is present as SAG, occurring as graphite laths and blocks, with δ^{13}C values ranging from−5 to 0 ‰ (Storz et al., 2021). These values closely align with the bulk δ^{13}C values of bulk EH (−7 ± 1 ‰) and EL (−2 ± 4 ‰) chondrites (Grady et al., 1986) (Fig. 2, Table 1). Note that similar to ordinary chondrites, the organic component in enstatite chondrites is thought to have originated from a common organic precursor shared with carbonaceous chondrites (Alexander et al., 1998). However, the ^{13}C-rich nature of graphite in enstatite chondrites relative to bulk δ^{13}C signature of ordinary chondrites suggests either that the organic matter underwent a completely different processing pathway due to their anomalously reduced characteristics, or that the graphite did not result from the thermal processing of organic precursors but instead originated through distinct nebular processes.

3.4. *Angrites, HEDs, aubrites, and iron meteorites*

Magmatic C in plutonic angrites ranges from ~ 2 to 140 μg/g. The δ^{13}C values of magmatic C in most plutonic angrites are lower than−20 ‰, with a mean value of−22 ± 3 ‰ (Fig. 2, Table 1) (Abernethy et al., 2013, 2018). In contrast, the δ^{13}C values of D'Orbigny, a vesicular angrite, are higher (−17 to−5 ‰). The correlated distinctly high δ^{13}C and δ^{15}N values of D'Orbigny relative to other plutonic angrites suggests that its heavier C isotopic composition results from open-system kinetic isotopic fractionation during degassing (Abernethy et al., 2013, 2018). Similar to angrites, HEDs, with magmatic C abundances of ~ 2–27 μg/g, exhibit distinctly low δ^{13}C values within a range of−30 to−19 ‰ (Grady et al., 1997b; Abernethy et al., 2018). No systematic differences in δ^{13}C values are observed amongst howardites, eucrites, and diogenites which sample surface materials, basaltic crust, and mantle, respectively, of the HED parent body (Grady et al., 1997b; Abernethy et al., 2018). The mean δ^{13}C value of HEDs (−25 ± 1 ‰) is slightly lower than that of angrites and is similar to ordinary chondrites (Fig. 2, Table 1). As with angrites, there are no systematic differences between the δ^{13}C values and C content within HEDs (Grady et al., 1997b; Abernethy et al., 2013, 2018). The δ^{13}C value of Bustee aubrite (−22 ‰) falls within a similar range to that of HEDs and angrites (Grady et al., 1986) (Fig. 2, Table 1). In contrast to basaltic achondrites, the C isotopic compositions of magmatic iron meteorites, which sample the metallic cores of the earliest solar system planetesimals, remain poorly constrained. The bulk δ^{13}C values of the taenite phase in two IIIAB irons (Welland = −21 ‰ and Joe Wright Mountain = −22 ‰) and one IIIE iron (Staunton = −20 ‰), all from the NC reservoir, are comparable to the those of angrites, HEDs, and aubrites (Deines and Wickman, 1975).

3.5. *Ureilites*

Ureilites contain up to ~ 6–8 wt% C (mean ~ 3.5 wt%), primarily in the form of graphite and minor amounts of high-pressure allotropes diamond and lonsdaleite (Grady et al., 1985; Goodrich et al., 1987; Russell et al., 1993; Smith et al., 2001; Downes et al., 2015; Barrat et al., 2017). Morphological similarities suggest that highly crystalline graphite, observed in minimally to moderately shocked samples, is the primary form of C in all ureilites (Grady et al., 1985; Storz et al., 2021). Textural relationships in coarse-grained ureilites, such as graphite filling interstitial sites between silicates and its close association with metal, indicate that graphite crystallized from a melt on the ureilite parent body (Goodrich et al., 1987, 2015). The δ^{13}C values of ureilites, predominantly in the coarse-grained graphite, cluster into two distinct groups around−8 ‰ and 0 ‰ (Barrat et al., 2017). The preservation of a well-defined relationship between olivine core compositions and δ^{13}C values suggests that the primary C isotopic compositions remained largely unaffected during the disruption of the ureilite parent body (UPB) (Barrat et al., 2017). The mean δ^{13}C values of bulk ureilites (−4 ± 1 ‰) is similar to enstatite chondrites (Fig. 2, Table 1), where graphite is the primary C-bearing phase, as well as that of graphite component in IAB irons (Deines and Wickman, 1973) and Winona (Grady and Pillinger, 1986), a primitive achondrite. Like enstatite chondrites, origin of the graphite component in ureilites remains poorly understood.

4. Effect of planetesimal processing on carbon isotopic compositions of chondrites

As noted in section 3, meteorite groups that sample both NC and CC reservoirs show substantial variations in their C isotopic compositions. These variations arise from the types of C-bearing phases present, such as organics, carbonates, graphite, and magmatic carbon, as well as the extent of parent body processing they underwent. Carbonaceous organics, the primary primordial C carrier in most of the chondrites, underwent complex evolutionary stages during parent body processing, including the degradation of simple organic molecules, polymerization into complex macromolecules, and/or the graphitization of IOM (Sephton et al., 2003; Alexander et al., 2007, 2017). In the more primitive carbonaceous chondrites (such as CI, CM, and CR), bulk C isotope ratios are strongly influenced by secondary carbonates. These carbonates formed during low-temperature aqueous alteration involving ^{13}C-rich fluids, which likely originated from CO_2-CO-rich ices (Alexander et al., 2015; Fujiya et al., 2019, 2023) (Fig. 3). Variations in their C isotopic composition may reflect differences in the ratio of ^{13}C-rich CO_2-CO ice to organics matter, potentially linked to the location of their parent body accretion in the early solar system. In contrast, CO and CV chondrites, which experienced significant thermal metamorphism, lack carbonates and consistently display lower δ^{13}C values (Fig. 2). It is uncertain whether these lower values reflect the absence of ^{13}C-rich ices at the time of accretion or the later destruction of pre-existing carbonates by heating. Whereas ureilites and enstatite chondrites, with crystalline graphite as the primary C carrier, display δ^{13}C values similar to those of carbonate-bearing CI, CM, and CR chondrites but significantly higher than those of carbonate-free CO, CV, and ordinary chondrites (Fig. 2). Magmatic C in basaltic achondrites and iron meteorites likely represents a high-temperature carrier that was present during the final stages of thermal metamorphism of chondrite-like materials and eventually participated in igneous processes (Grewal et al., 2021a, 2022a; Grewal, 2022). Given the diversity of the C carriers and the varying degrees of parent body processing they experienced, it is crucial to explore the C isotopic composition variations in meteorites within a unified framework of parent body processing. This approach can help establish potential connections between the C isotopic compositions of the BSE, Martian meteorites, and the early solar system planetesimals sampled by different meteorite groups.

Thermal evolution of early solar system planetesimals was controlled by ^{26}Al, a short-lived radionuclide with a half-life of ~ 0.7 Myr. It was present in sufficient quantities in the early solar system to cause large-scale melting and differentiation (Hevey and Sanders, 2006; Sahijpal et al., 2007). Consequently, the peak temperatures experienced by the early planetesimals were largely determined by their accretion timescales. For instance, the accretion ages of the parent bodies of magmatic iron meteorites and achondrites, which underwent complete differentiation, are older than those of partially differentiated primitive achondrites, which, in turn, have older accretion ages than undifferentiated chondrite parent bodies (Sugiura and Fujiya, 2014; Kruijer et al., 2014). Iron meteorites and other differentiated achondrites therefore likely record the final stages of thermal evolution within the interiors of planetesimals that initially accreted chondritic material (Grewal et al., 2022a, 2025a, 2025b; Grewal and Asimow, 2023). Among the chondrite parent bodies, the more thermally metamorphosed enstatite, ordinary, and CO and CV chondrites exhibit older accretion ages compared to the more primitive CI, CM, CR, and Tagish Lake chondrites (Sugiura and Fujiya, 2014). Additionally, spatial variations in the growth zones of early planetesimals could have led to the accretion of materials with varying ice-to-rock ratios, resulting in differing exposures to aqueous alteration (Lichtenberg et al., 2019, Lichtenberg et al., 2021; Grewal et al., 2024b). For instance, CI and CM chondrites, originating from the outer regions of the disk, bear evidence for extensive aqueous alteration on their parent bodies (Brearley, 2006; Alexander et al., 2012). Carbonates, which are key products of this alteration, play an important role in defining the bulk C isotopic compositions of chondrites that sample such planetesimals (Fig. 3).

To better understand the influence of parent body processing on the bulk C isotopic compositions of planetesimal reservoirs, we follow the approach used in previous studies, tracking variations in C and N abundances, as well as N isotopic compositions, across chondrites and achondrites as a function of a common thermal index (Grewal, 2022; Grewal et al., 2022a, 2025a). The thermal evolution of carbonaceous, ordinary, and enstatite chondrites can be monitored using their peak metamorphic temperatures (T_{eff}), inferred through organic thermometry of IOM (Cody et al., 2008). Volatile-rich chondrites such as CI, CM, CR, and Tagish Lake exhibit peak metamorphic temperatures below 200 °C (Fig. 5). Moderately metamorphosed CO, CV, and type 3 ordinary chondrites show peak metamorphic temperatures between 200 and 600 °C, while Indarch, an EH4 enstatite chondrite, exhibits a peak

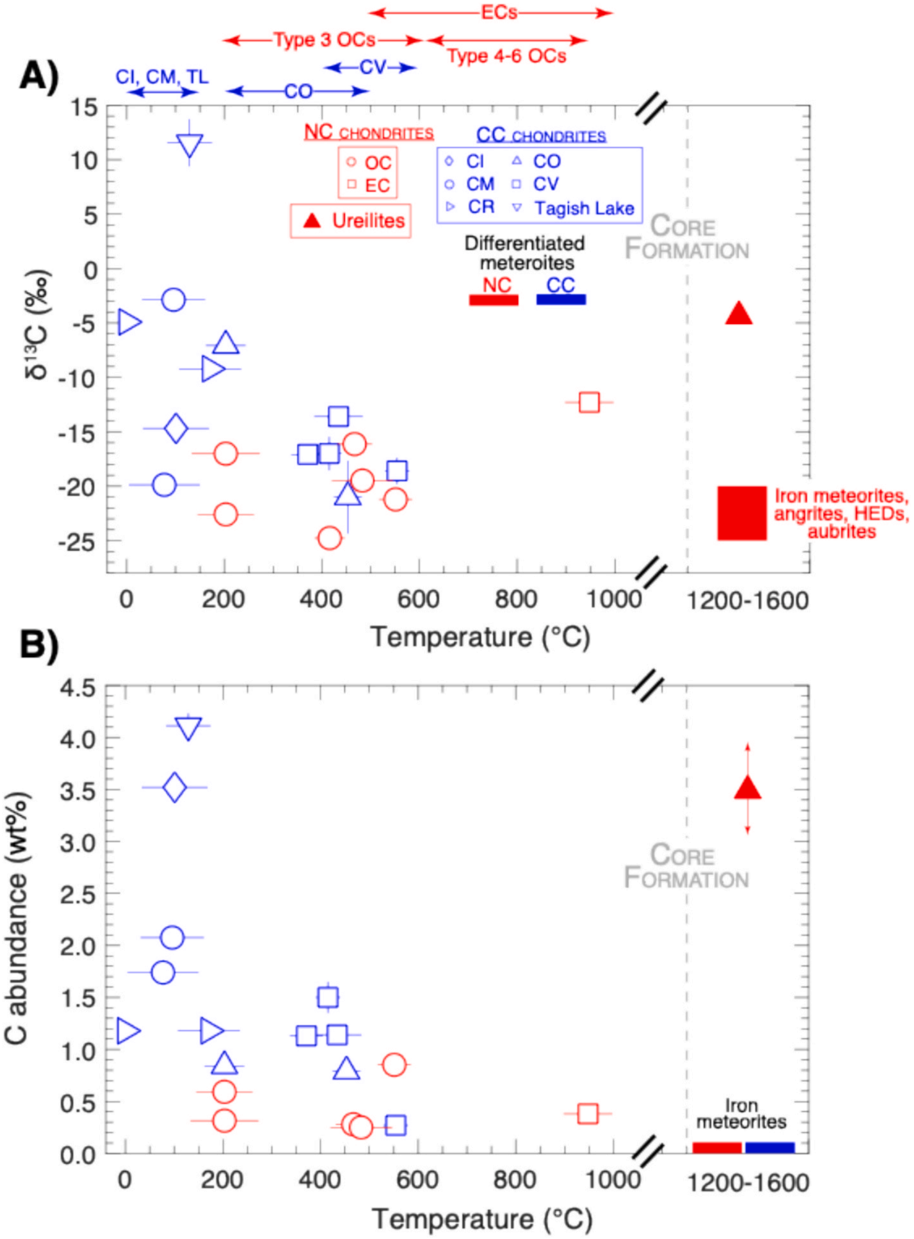

Fig. 5. (A) $\delta^{13}C$ values and (B) carbon abundances of chondrites and differentiated meteorites plotted as a function of their peak metamorphic temperatures (T_{eff}). Chondrites from both NC and CC reservoirs, except enstatite chondrites, show a trend of decreasing $\delta^{13}C$ values and C content with increasing T_{eff}. Differentiated meteorites, except ureilites, exhibit low $\delta^{13}C$ values and C abundances which follow the trend of thermally metamorphosed chondrites. Data: T_{eff} – (Cody et al., 2008); C abundance and $\delta^{13}C$ values and the relevant references are reported in Table 1 and Supplementary Table 1.

metamorphic temperature of ~ 950 °C (Cody et al., 2008). Except for Indarch, these organic thermometry values align well with independent estimates of peak metamorphic temperatures for chondrites using petrological and geochemical proxies (indicated by arrows above Fig. 5A). For instance, type 3 ordinary chondrites reach peak metamorphic temperatures between 200 and 600 °C, whereas types 4–6 reach temperatures between 600 and 950 °C (Huss et al., 2006; Monnereau et al., 2013). Type 4 enstatite chondrites exhibit peak metamorphic temperatures of 500–650 °C, and types 5–6 range between 600 and 1000 °C. CO and CV chondrites fall within the range of 200–500 °C and 400–600 °C, respectively (Yesiltas et al., 2021). CI and CM chondrites exhibit significantly lower peak temperatures, typically ranging from 0 to 100 °C (Huss et al., 2006; Guo and Eiler, 2007; Clog et al., 2024), though some estimates suggest that CM chondrites may have experienced temperatures as high as 150 °C (Vacher et al., 2019b, a; Verdier-Paoletti et al., 2019). Meanwhile, ureilites experienced igneous processing at temperatures of up to 1200–1300 °C (Goodrich et al., 2015). Angrites, HEDs, aubrites, and magmatic irons sample planetesimal reservoirs that likely experienced temperatures as high as 1400–1600 °C due to large-scale melting and core-mantle differentiation in their parent bodies (Kruijer et al., 2014, 2017; Steenstra et al., 2019).

Based on T_{eff}, the δ^{13}C values of Tagish Lake, CI, CM, CR, CO, CV, and ordinary chondrites show distinct groupings that correspond to their thermal history (Fig. 5**A**). At $T_{\mathrm{eff}} < 200$ °C, Tagish Lake, CI, CM, and CR chondrites show significant variations in C isotopic compositions, with δ^{13}C values ranging from −20 to 12 ‰. As discussed earlier, this variation is primarily controlled by the presence of ^{13}C-rich carbonates (Fig. 3). CO, CV, and ordinary chondrites, with $200 < T_{\mathrm{eff}} < 600$ °C, display δ^{13}C values within a relatively narrower range of −25 to −14 ‰. The C abundances in these chondrites also follow a similar trend, with lower bulk C contents observed at higher T_{eff} (Fig. 5**B**). Similar trends have also been observed for N abundances and δ^{15}N values with T_{eff}, with both decreasing at higher T_{eff} (Grewal, 2022; Grewal et al., 2022a, 2025a). The similarity in δ^{13}C values and C abundances between type 3 ordinary chondrites and CO and CV chondrites suggests that ordinary chondrites could have accreted organic precursors similar to those in carbonaceous chondrites. In fact, C-rich aggregates, the primary carrier of C in ordinary chondrites, are believed to have originated from the thermal processing of carbonaceous material in the parent bodies of ordinary chondrites (Scott et al., 1987; Grady et al., 1989; Alexander et al., 1998). The overall lower mean δ^{13}C values of ordinary chondrites compared to CO and CV chondrites can be attributed to inclusion of the more thermally metamorphosed type 4–6 ordinary chondrites, which have consistently lower δ^{13}C values than unequilibrated type 3 ordinary chondrites (Fig. 4**B**). Angrites, HEDs, aubrites, and NC iron meteorites exhibit uniformly low δ^{13}C values, which fall within the range of C isotopic compositions of ordinary, CO, and CV chondrites (Fig. 5**A**). However, the δ^{13}C values in graphite-bearing ureilites and enstatite chondrites, despite their high peak metamorphic temperatures, are distinctly higher.

What causes the high δ^{13}C values observed in ureilites and enstatite chondrites, despite their extensive thermal processing? At this stage, there is no definitive answer to this question. As mentioned earlier, graphite in meteorites can originate as a product of thermal metamorphism of organic matter. On chondrite parent bodies, thermal metamorphism can cause carbonaceous material to crystallize into graphite, a process that occurs during the heating of the parent body, typically at temperatures of ~ 400–800 °C (Scott et al., 1987; Grady et al., 1989). The similarity in the C isotopic compositions of CO and CV chondrites, where C is predominantly present in the IOM component, and ordinary chondrites, where C exists as poorly graphitized carbon, suggests that graphitization may indeed occur during the thermal metamorphism of organic matter. However, if the graphite in ureilites and enstatite chondrites, where it is almost entirely in the crystalline form, formed through similar processes, their C isotopic compositions would be expected to follow trends observed in other NC and CC meteorites (Fig. 5**A**). However, they do not. Notably, ureilites are anomalously C-rich for primitive achondrites, while enstatite chondrites are also more C-rich compared to other thermally metamorphosed chondrites (Fig. 5**B**). The hyperbolic relationship between the C isotopic composition of graphite in coarse-grained ureilites and olivine compositions suggests that the UPB accreted from two isotopically distinct C-rich precursors, which did not fully mix on the UPB (Barrat et al., 2017). Thus, the C isotopic composition of graphite in ureilites likely reflects a primordial signature rather than one produced by parent body processing. Graphite clasts in ordinary chondrites, although a minor host of C, display δ^{13}C values within the range of the graphite component in ureilites and enstatite chondrites (Storz et al., 2021). Thus, the distinct C isotopic composition of the graphite component in ureilites and enstatite chondrites may reflect precursors with formation histories different from those of the organic precursors. However, we note that this remains a tentative hypothesis, and additional work is required to better understand the origin of the C isotopic composition of graphite in ureilites and enstatite chondrites.

In summary, parent body processing likely played a significant role in shaping the bulk C isotopic compositions of meteorites. The C isotopic compositions of Tagish Lake, CI, CM, CR, CO, CV, and ordinary chondrites can be attributed to the varying effects of parent body processing of common C precursors. In Tagish Lake, CI, CM, and CR chondrites, variations in C isotopic compositions are influenced by the presence of a ^{13}C-rich carbonate component, which can be ~ 60–80 ‰ heavier than the organic component. In the more thermally metamorphosed CO, CV, and ordinary chondrites, C isotopic compositions are dominated by the organic component, specifically IOM, which becomes progressively ^{13}C-depleted, particularly in ordinary chondrites as thermal metamorphism increases from type 3 to types 4–6. Similarly, basaltic achondrites, such as angrites, HEDs, and aubrites, as well as magmatic iron meteorites, exhibit ^{13}C-poor compositions. In contrast, ureilites and enstatite chondrites, where nearly all C is present as crystalline graphite of currently unknown origins, display ^{13}C-enriched compositions, similar to those of some ^{13}C-rich carbonaceous chondrites.

5. Origin of carbon in BSM and BSE

Although the cause(s) of some intergroup variations in the C isotopic compositions of meteorites remain debated (Alexander et al., 2007, 2017; Lawrence et al., 2025), the overall range of these variations can be used to place first-order constraints on the origin of C in terrestrial planets. Since terrestrial planets are formed from planetesimals – differentiated and/or undifferentiated – rather than directly from primordial materials in the disk (Burkhardt et al., 2021; Morbidelli et al., 2025), a lack of complete understanding of the parent body processes affecting the evolution of C isotopic compositions in planetesimals relative to the primordial accreted materials does not necessarily pose a hindrance. This is true as long as the C isotopic variations observed in undifferentiated, partially differentiated, and fully differentiated meteorites adequately represent the variations in the C isotopic compositions of the building blocks of terrestrial planets, sourced from both the inner and outer regions of the disk. While some degree of intra-group variability in the C isotopic compositions of meteorites, particularly chondrites, exists, this variability is smaller than the inter-group differences in their C isotopic compositions. For instance, although the δ^{13}C values of ordinary chondrites (H, L, and LL) vary between −30 and −20 ‰ based on their metamorphic scale (Fig. 4**B**), their mean δ^{13}C values are distinct from those of other chondrite classes (Fig. 2). Therefore, the mean δ^{13}C values of meteorites can serve as a valuable tool for placing first-order constraints on the origin of C in terrestrial planets.

The mean δ^{13}C values of NC meteorites fall within a narrow range of −25 to −20 ‰, with the exception of ureilites and enstatite chondrites, whose δ^{13}C values resemble those of volatile-rich carbonaceous chondrites (Fig. 2). The mean δ^{13}C values of ordinary chondrites (H, L, and LL) overlap with those of several differentiated achondrites that sample both silicate (e.g., angrites, HEDs, and aubrites) and metallic reservoirs (e.g., magmatic iron meteorites). Notably, these values also overlap with the mean $\delta^{13}C$ value of Martian meteorites. Meanwhile, the $\delta^{13}C$ value of the BSE overlaps with those of both NC and CC meteorites. For instance, the canonical $\delta^{13}C$ value of BSE is nearly identical to that of enstatite chondrites and ureilites from the NC reservoirs and falls within the range of relatively primitive CI, CM, and CR chondrites from the CC reservoir (Fig. 2), although recent studies suggest that BSE $\delta^{13}C$ value could be slightly lower (Moussallam et al., 2025a, b; Moussallam, 2025). At face value, this suggests that the distinct $\delta^{13}C$ values of Martian meteorites and BSE, combined with their resemblance with different groups of NC and CC meteorites, may reflect differences in their volatile accretion histories.

Before exploring the cosmochemical implications of this observation, an important question must be addressed: do the distinctly lower $\delta^{13}C$ values of Martian meteorites suggest that the bulk $\delta^{13}C$ value of the BSM is lower than that of the BSE? Or do these values indicate that the magmatic C measured in Martian meteorites has been influenced by isotope fractionation during magma degassing or emplacement, involving volatile loss from a primordial component which had a BSE-like initial $\delta^{13}C$ value? At the oxygen fugacity (fO_2) relevant for shergottite petrogenesis (~IW + 1) (Nicklas et al., 2021), CO_3^{2-} is the dominant C species in silicate melts (Stanley et al., 2011, 2012; Li et al., 2017). Experimental data and theoretical models have shown that equilibrium and kinetic C isotope fractionation ($\Delta^{13}C^{vap-melt}$) between vapor (CO_2) and mafic melt (CO_3^{2-}) operate in opposite directions: $\Delta^{13}C_{eq}^{vap-melt}$ is positive, meaning the residual melt is lighter than the vapor during equilibrium fractionation, while $\Delta^{13}C_{kinetic}^{vap-melt}$ is negative, making the residual melt heavier than the vapor during kinetic fractionation (Javoy et al., 1978; Mattey et al., 1990; Mattey, 1991; Aubaud, 2022; Lee et al., 2024). Evidence for both equilibrium and kinetic fractionation of C isotopes exists during the degassing of terrestrial basalts. For instance, the low $\delta^{13}C$ values (between −25 and −5 ‰) observed in the most C-poor terrestrial basalts have generally been explained by Rayleigh fractionation under equilibrium conditions (Aubaud, 2022). However, recent measurements of C isotopic compositions in volcanic gases and melt inclusions during the 2021 Fagradalsfjall eruption suggest that kinetic CO_2 degassing during magma ascent may be more common than previously thought (Moussallam et al., 2024). The combined systematics of C and noble gas contents of MORBs also indicate a significant role of kinetic disequilibrium during magma degassing (Tucker et al., 2018).

If the C isotopic compositions of magmatic C in Martian meteorites were influenced by kinetic fractionation during degassing, the $\delta^{13}C$ values of their source, and by extension the Martian mantle, could be lower than those measured in the meteorites. These lower values, potentially overlapping with those of ^{13}C-poor type 4–6 ordinary chondrites, basaltic achondrites, and iron meteorites (Fig. 2), would further distinguish the $\delta^{13}C$ value of the BSM from that of the BSE. Conversely, if degassing occurred via Rayleigh fractionation under equilibrium conditions, the $\delta^{13}C$ value of the Martian mantle could be significantly higher, potentially resembling that of the BSE. However,

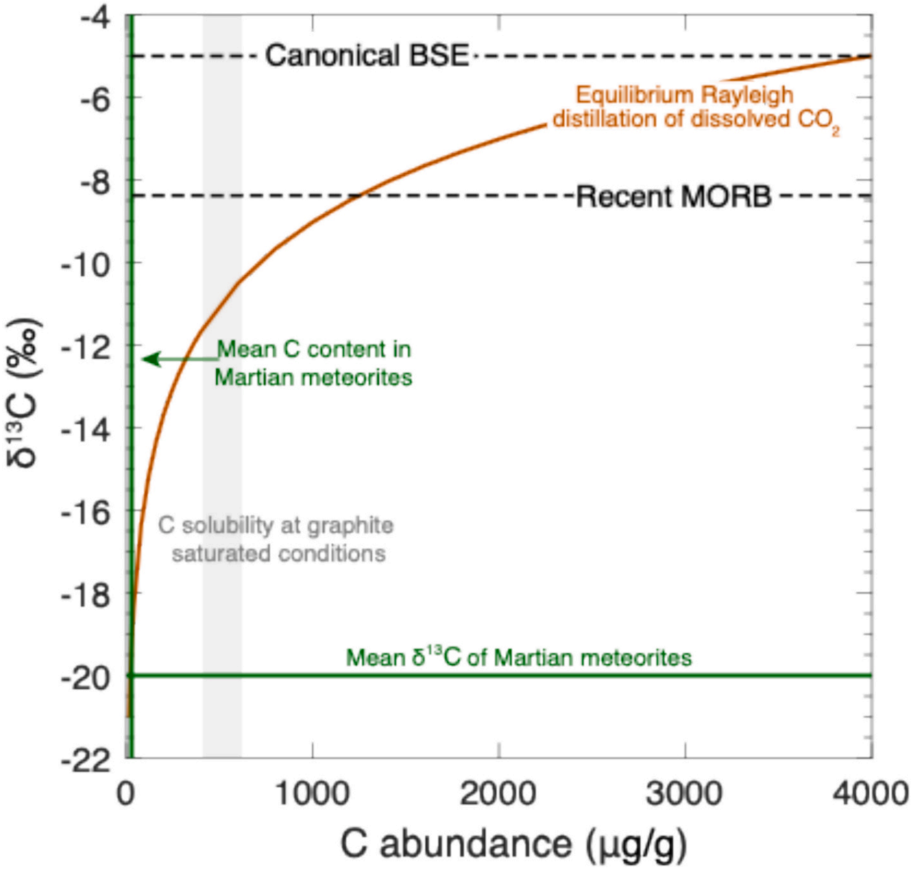

Fig. 6. Modeled $\delta^{13}C$ evolution of Martian magmas undergoing equilibrium Rayleigh distillation of dissolved CO_2 as a function of residual C abundance in the melt. The curve is based on an initial $\delta^{13}C$ value of −5 ‰ (representative of the BSE) and an experimentally determined $\Delta^{13}C_{eq}^{vap-melt}$ value of + 2.9 ‰) (Lee et al., 2024). The shaded vertical band denotes the estimated solubility limit of C in mafic melts under graphite-saturated conditions at fO_2 relevant to petrogenesis (~IW + 1). The mean $\delta^{13}C$ value and C content of Martian meteorites are marked with green solid lines for reference. The model shows that even under C solubility limit at graphite saturated conditions, Rayleigh fractionation under equilibrium conditions from a BSE-like source cannot account for the $\delta^{13}C$ values observed in Martian meteorites, suggesting a more ^{13}C-depleted Martian mantle source.

the scarcity of C isotope data for Martian basalts, especially in comparison to terrestrial basalts, limits our ability to evaluate whether such equilibrium processes fractionated δ^{13}C values from a BSE-like mantle source.

Using the mean C abundance in Martian meteorites (~20 μg/g) and the recently determined experimental value for $\Delta^{13}\,\mathrm{C}_{\mathrm{eq}}^{\mathrm{vap-melt}}$ of + 2.9 ‰ in mafic melts with NBO/T (non-bridging oxygen per tetrahedral cation) greater than 0.88 (Lee et al., 2024), an undegassed parent magma would require ~ 4000 μg/g C to generate the observed δ^{13}C values through Rayleigh fractionation under equilibrium conditions from a mantle source with the canonical BSE-like δ^{13}C value of −5 ‰ (Fig. 6). In contrast, a lower BSE δ^{13}C value (−8.4 ‰) would require a lower parent magma C content of ~ 1000 μg/g. For C-rich samples like Dhofar 019 and Zagami, the required C content would exceed 1 wt%. All of these values are higher than the graphite-saturated C solubility limit in silicate melts (~500–600 μg/g) at the fO_2 relevant for shergottite petrogenesis (IW + 1) (Li et al., 2017). Importantly, the graphite-saturated limit defines the maximum possible C content in Martian parent magmas. If the mantle was graphite-undersaturated, as is more likely, then the C content would have been even lower (Li et al., 2017). Even at the upper solubility limit, the required δ^{13}C value of the parent magma would range from −12 to − 10 ‰, which is significantly lower than the canonical BSE value of −5 ‰ but closer to the recently proposed MORB mantle value of −8.4 ‰. Coincidentally, this estimate is strikingly similar to the δ^{13}C value of bulk Mars (−10.5 ‰), based on its proposed building blocks by Dauphas et al. (2024): a mixture of two-thirds enstatite chondrite-like and one-third ordinary chondrite-like material (based on nucleosynthetic anomalies) with similar C contents. However, we caution that this apparent similarity may simply result from the extreme assumptions of maximum C solubility and equilibrium–controlled Rayleigh degassing.

While the preceding discussion suggests that Rayleigh fractionation under equilibrium conditions could significantly lower the δ^{13}C value of Martian meteorites relative to the mantle source, the scenario relies on idealized assumptions about C content in parent melts and degassing efficiency. In contrast, several independent lines of evidence suggest that degassing processes may not have strongly fractionated C isotopes in Martian meteorites, and that their δ^{13}C values may more closely reflect those of the Martian mantle source:

1) The δ^{13}C values of less degassed Martian shergottites fall within the range of those more extensively degassed. For instance, Dhofar 019 and Zagami, which have C contents ~ 1–2 orders of magnitude higher than other Martian meteorites, display δ^{13}C values that overlap with the extensively degassed samples (Grady et al., 2004). Unlike terrestrial basalts, where Rayleigh fractionation under equilibrium conditions systematically lowers δ^{13}C values as C content decreases (Aubaud, 2022), there is no correlation between the C content and isotopic compositions of Martian meteorites.
2) The C abundances of three other basaltic meteorites, i.e., angrites, HEDs, and aubrites, are almost identical to those in Martian meteorites (Fig. 2). However, unlike Martian meteorites, these three groups originate from planetesimal-sized bodies and must have experienced different degassing histories compared to a planet-sized body. Notably, the large variability in the fO_2 of their magma petrogenesis (aubrites = IW − 6; HEDs = IW − 2; angrites = IW + 1 (Righter et al., 2016)) means that the speciation of C in their magmas, particularly aubrites and HEDs, would be dominated by molecular CO and CH_4, rather than CO_3^{2-} (Yoshioka et al., 2015, 2019; Li et al., 2017; Keppler and Golabek, 2019; Grewal et al., 2020, 2021a). While the $\Delta^{13}\,\mathrm{C}_{\mathrm{eq}}^{\mathrm{vap-melt}}$ values for CO and CH_4 degassing are currently unknown, they could differ significantly – both in magnitude and direction – from the $\Delta^{13}\,\mathrm{C}_{\mathrm{eq}}^{\mathrm{vap-melt}}$ of CO_3^{2-} degassing. This is because degassing of CO and CH_4 from silicate melts, unlike that of CO_3^{2-}, entails a transition from a molecular species in the silicate melt to a molecular species in vapor (Fine and Stolper, 1985, 1986; Holloway et al., 1992; Yoshioka et al., 2015, 2019). The remarkable similarity in the C isotopic compositions of angrites, HEDs, and aubrites to those of Martian meteorites, despite substantial differences in their petrogenesis and degassing histories, suggests that their C isotopic compositions may reflect the δ^{13}C values of their source mantles.
3) The bulk C isotopic compositions of NC magmatic irons (IIIAB and IIIE groups) are almost identical to those of angrites, HEDs, and aubrites as well as Martian meteorites (Fig. 2). Although equilibrium C isotope fractionation between metallic and silicate melts remains unconstrained, theoretical calculations (Horita and Polyakov, 2015) and comparable experimental data (e.g., C isotope fractionation between graphite and silicate or metallic melts (Satish-Kumar et al., 2011; Mizutani et al., 2014), and N isotope fractionation between metallic and silicate melts (Grewal et al., 2022b)) suggest limited C isotope fractionation at the high temperatures relevant to core-mantle differentiation. Unlike basaltic achondrites, the C isotopic compositions of NC magmatic irons do not reflect any degassing effects during magma ascent. Therefore, the remarkable similarity in their isotopic compositions suggests that the C isotopic compositions of magmatic C in early formed differentiated objects in the inner solar system likely lay within a narrow range.

In conclusion, if C isotopic fractionation during degassing was limited or dominated by kinetic processes, the bulk δ^{13}C value of the BSM, as inferred from Martian meteorites (≤−20 ‰), would be significantly lower than that of the canonical estimate of the BSE (−5‰). In this scenario, the similarity in δ^{13}C values between Martian meteorites and other differentiated planetary materials, such as angrites, HEDs, aubrites, and NC magmatic irons, reveals a remarkable consistency in the C isotopic compositions of igneous reservoirs in early differentiated inner solar system bodies (Fig. 2). Interestingly, the δ^{13}C values of ordinary chondrites fall within this same range, while those of enstatite chondrites and ureilites are distinctly higher. The similarity of δ^{13}C values in Martian meteorites, basaltic achondrites, and NC irons with trends defined by T_{eff} (Fig. 5**A**) suggests that their C likely originated from a thermally metamorphosed endmember of carbonaceous organics. This source would be isotopically distinct from the graphite-rich reservoirs sampled by enstatite chondrites and ureilites. Given that Mars, like angrites, HEDs, and aubrites, formed exclusively from NC materials and accreted its MVE inventory from the same reservoir (Burkhardt et al., 2021; Paquet et al., 2023; Kleine et al., 2023), the similarity in C isotope composition among these differentiated objects supports the interpretation that Mars acquired its C from locally sourced NC materials. In this framework, ordinary chondrites may represent the undifferentiated counterparts of these materials in C isotope space.

Alternatively, if Martian meteorites experienced extensive Rayleigh fractionation under equilibrium conditions during degassing, then the δ^{13}C value of the BSM would be higher than that recorded in the meteorites. However, even under the most extreme scenario – Rayleigh degassing from a graphite-saturated melt – the δ^{13}C value of the BSM would be constrained to −12 to −10 ‰. This is still lower than the canonical BSE value of −5 ‰ but closer to the recently proposed MORB mantle value of −8.4 ‰. In that case, the C isotopic composition of the BSM could reflect a mixture of ^{13}C-poor and ^{13}C-rich precursors. A ~ 1:2 mixture of ordinary and enstatite chondrite-like materials, consistent with the compositional building blocks inferred from nucleosynthetic anomalies in non-volatile elements, could account for the observed δ^{13}C signature of the BSM.

Meanwhile, the canonical δ^{13}C value of the BSE is comparable to that of enstatite chondrites and ureilites from the NC reservoir and volatile-rich CI, CM, and CR chondrites from the CC reservoir (Fig. 2). This suggests that the C source in the BSE could derive from either NC or CC materials. For the former, the C source would be the thermally stable graphite component, while for the latter, it would be the matrix component, which is easily altered. Unlike Mars, nucleosynthetic anomalies of Zn (a MVE whose abundance correlates with C in carbonaceous chondrites; Fig. 1) suggest that Earth accreted ~ 30 % of its Zn from the CC reservoir (Steller et al., 2022; Savage et al., 2022; Martins et al., 2023). To reconcile the contribution of Zn with other non-volatile elements, ~5% of Earth's CC mass must have been delivered by volatile-rich CI chondrite-like materials (Steller et al., 2022). Combined with the isotopic signatures of non-volatile siderophile elements and Pd-Ag isotope systematics, these materials were most likely delivered during the final stages of Earth's accretion (Schönbächler et al., 2010; Nimmo et al., 2024). Considering the C-depleted nature of the BSE, such late delivery of CC materials could account for its entire C inventory (Marty, 2012; Halliday, 2013), but would require that some CC-derived C was either sequestered into the core or lost to space (Grewal et al., 2024a; Grewal and Manilal, 2025). Importantly, these CC materials are also rich in N and H. Thus, in addition to supplying C, primitive carbonaceous materials could have contributed the entire N–H inventory of the BSE (Marty, 2012; Alexander et al., 2012; Halliday, 2013), although the superchondritic C/N ratio in the BSE remains a challenging problem to explain (Marty, 2012; Tucker and Mukhopadhyay, 2014; Hirschmann, 2016; Grewal et al., 2019b; Dasgupta and Grewal, 2019; Marty et al., 2020; Grewal and Asimow, 2023). If the C isotopic signature of the BSE reflects delivery from enstatite chondrite- and ureilite-like materials, accounting for its H inventory is difficult, as ureilites are extremely H-poor (Peterson et al., 2023b). Although some recent work has suggested high H contents in enstatite chondrites (Piani et al., 2020; Thomassin et al., 2023; Barrett et al., 2025), these findings may still reflect terrestrial contamination (Peterson et al., 2023a; Ordonez et al., 2024), and enstatite chondrites might indeed be intrinsically H-poor. This suggests that the heavier C isotopic composition of the BSE relative to BSM likely reflects a bias toward the late delivery of volatile-rich carbonaceous materials. These materials could have been delivered by Moon-sized CC bodies during the late stages of Earth's accretion (not to be confused with "late accretion") (Dauphas et al., 2024; Nimmo et al., 2024). However, if the recently proposed lower δ^{13}C value of the MORB mantle (−8.4 ‰) is representative of the BSE, then ^{13}C-rich CI, CM, and CR chondrites cannot be its exclusive C source, and an additional ^{13}C-poor component is required (Fig. 2). Although CV and CO chondrites meet this criterion, the ^{13}C-poor contribution was more likely derived from the NC reservoir, which supplied ~ 95 % of Earth's mass. Taken together, our findings suggest that the C inventory of the BSE was dominated by late-delivered, ^{13}C-rich CC materials. This contrasts with the NC-derived, ^{13}C-poor inventory of BSM, underscoring how the different growth histories of Earth and Mars shaped their volatile budgets.

6. Implications for the carbon isotopic composition of the bulk Earth

As discussed in the previous section, the canonical C isotopic composition of the BSE, consistent with its C-depleted inventory, likely reflects the accretion of relatively primitive carbonaceous materials during the later stages of Earth's growth. But what about the C isotopic signatures of materials accreted during the earlier, more substantial phases of Earth's formation? Planet formation models suggest that Earth's major building blocks – differentiated planetesimals and planetary embryos – formed rapidly after the solar system's formation (Weidenschilling, 2019). Since ~ 95 % of Earth's mass is NC in composition, these differentiated bodies must be predominantly made of NC materials (Dauphas, 2017; Burkhardt et al., 2021; Dauphas et al., 2024). The striking similarity in the C isotopic composition of Martian meteorites – sampling a planetary embryo that grew rapidly from locally sourced NC materials – and angrites, HEDs, aubrites, and magmatic iron meteorites – sampling early formed NC planetesimals – implies that the primary building blocks of Earth may also have exhibited similarly light C isotopic compositions ($\delta^{13}C = -25$ to −20 ‰) (Fig. 2). However, evidence from NC chondrites and primitive achondrites presents a more complex picture. While ordinary chondrites (H, L, and LL groups) display δ^{13}C values (−25 ‰) similar to other early inner solar system differentiated objects, enstatite chondrites and ureilites, which contain graphite as the primary C carrier, show heavier C isotopic values (δ^{13}C ~ − 5 ‰). These heavier values overlap with the canonical C isotopic composition of the BSE.

Nucleosynthetic anomalies in several non-volatile elements suggest that enstatite chondrites represent the average isotopic composition of NC materials accreted by Earth (Dauphas, 2017; Dauphas et al., 2024). Considering the C isotopic compositions of enstatite chondrites and the BSE, it appears at face value that Earth could have accreted materials with a δ^{13}C value of −5 ‰ throughout its growth. Since minimal fractionation of C isotopes is expected under the high-temperature conditions relevant for core-mantle differentiation, this would suggest that the δ^{13}C value of the bulk Earth is also close to −5 ‰. However, this prediction is at odds with the δ^{13}C values observed in Martian meteorites and other early differentiated NC planetesimals, except for graphite-bearing ureilites. Previous studies have repeatedly emphasized that Earth's isotopic similarity to enstatite chondrites does not necessarily imply that Earth accreted materials compositionally identical to enstatite chondrites (Dauphas, 2017; Dauphas et al., 2024). This distinction is particularly important for C, as enstatite chondrites are highly reduced, and the graphite they contain may have originated through other processes, such as nebular condensation in an anomalously reduced environment. Although the exact contribution of graphite-bearing enstatite chondrite- and ureilite-like materials with δ^{13}C values around −5 ‰ to Earth's building blocks cannot currently be quantified, it is highly likely that relatively ^{13}C-poor differentiated bodies, similar to Mars and other early differentiated planetesimals, made a significant contribution to Earth's growth.

Where is the evidence of such ^{13}C −poor materials in Earth's rock record? Observations indicate that the C isotopic compositions of mantle xenoliths are heterogeneous, ranging from −30 to 0 ‰ (Cartigny et al., 1998; Deines, 2002; Cartigny, 2005). Notably, these values show a bimodal distribution with two prominent peaks: a sharp peak at −5 ‰, thought to represent the primordial C isotopic composition of Earth's mantle, and another distinct peak at −25 ‰ (Deines, 2002). The −25 ‰ peak aligns with the C isotopic composition of organic material, suggesting it reflects a subduction signature (Cartigny et al., 1998). This interpretation posits that carbonates are efficiently released at subduction zones, while organic material is preferentially subducted (Deines, 2002). Over Earth's history, the preferential subduction of organic C may have played a significant role in shaping the bimodal distribution of C isotopic compositions in the mantle. However, the −25 ‰ peak in Earth's mantle also closely aligns with the C isotopic composition of early differentiated inner solar system objects and ordinary chondrites. Whether this alignment is coincidental or reflects a fundamental connection is an open question. At present, most evidence linking the light C isotopic signatures in the Earth's mantle exclusively with subducted organic C is circumstantial and model dependent. As such, the possibility that some of the heterogeneity in the mantle C isotopic composition has a primordial origin cannot be dismissed outright. For this possibility to be unfounded would require either the efficient segregation of early accreted lighter C into Earth's core or its significant loss during impact events.

Recent studies using *in-situ* C isotope measurements in CO_2 undersaturated basalt glasses and melt inclusions have revelated that the δ^{13}C values of the MORB mantle are heterogenous (−10 to −4 ‰) (Moussallam et al., 2025a, b; Moussallam, 2025). While samples from Atlantic display δ^{13}C values similar to the canonical MORB mantle, those from the Arctic, Indian, and Pacific basins display lower values, with a mean value of −8.4 ‰ (Moussallam et al., 2025a, b). These observations led the authors to propose that this that this heterogeneity could reflect subduction process but may also be primordial in nature, suggesting that the δ^{13}C values of the BSE may be lower than the canonical estimate (Moussallam et al., 2025b). Given that Earth accreted primarily from NC materials during its main growth phase, and that these materials were likely differentiated and exhibited δ^{13}C values similar to meteorites that sample early solar system planetesimals and planetary embryos, it is plausible that the heterogeneity observed in the MORB mantle's C isotopic composition is indeed of primordial origin. As a result, the δ^{13}C value of the BSE is likely lower than the canonical value, although the exact value would depend on the sizes and contributions of these heterogenous reservoirs to Earth's overall mantle C budget. Noble gas isotopes and variations in N and H isotopic compositions also provide evidence for the existence of primordial volatile reservoirs in Earth's mantle (Cartigny and Marty, 2013; Piani et al., 2020; Péron et al., 2021).

The lighter C isotopic compositions of NC-differentiated meteorites also have important implications for the C isotopic composition of Earth's core. During Earth's collisional growth, differentiated planetesimals and planetary embryos, whose cores largely merged with the proto-Earth's core without undergoing significant metal-silicate equilibration in proto-Earth's magma ocean (Deguen et al., 2014; Landeau et al., 2021), contributed substantially to Earth's mass. Consequently, the C isotopic composition of Earth's core should predominantly reflect the lighter C isotopic signature of these early differentiated bodies. While some isotopically heavier C may also have partitioned into Earth's core, the overall isotopic composition is likely biased toward lighter values, given that the majority of Earth's mass originated from these sources. This accretion history of C suggests that the C in Earth's core may be isotopically out of equilibrium with the mantle. Similar to helium (Mundl-Petermeier et al., 2020; Horton et al., 2023) and H (Dottin et al., 2025), the exsolution of lighter C from Earth's core during cooling could release isotopically light C at the core-mantle boundary, which could also contribute the C isotope heterogeneity in Earth's mantle.

7. Conclusions

In this study we examined the relationship between the C isotopic compositions of planetary and planetesimal reservoirs to gain new insights into the origin of volatiles on Earth and Mars from a comparative planetology perspective. The magmatic C in Martian meteorites exhibits a distinctly lower mean δ^{13}C value (−20 ‰) compared to the canonical BSE estimate (−5‰). Several meteorites sampling the silicate and metallic reservoirs of early differentiated NC planetesimals, including angrites, HEDs, aubrites, and magmatic irons, also display δ^{13}C values overlapping with those of Martian meteorites. The C isotopic compositions of ordinary chondrites fall within a comparable range. Among carbonaceous chondrites, the δ^{13}C values of relatively primitive CI, CM, and CR chondrites overlap with that of the BSE. Crystalline graphite-bearing enstatite chondrites and ureilites, both from the NC reservoir, also exhibit δ^{13}C values that align with the C isotopic composition of the BSE. A shared correlation between δ^{13}C values and the peak temperatures of CC chondrites and several NC meteorites, including ordinary chondrites, basaltic achondrites, and irons, suggests that variations in their C isotopic compositions are primarily driven by the effects of parent body processing on common precursors. The distinct ^{13}C-rich composition of graphite-bearing enstatite chondrites and ureilites, despite their exposure to high peak temperatures, may stem from precursors that formed through distinct mechanisms.

If Martian magmas experienced minimal C isotopic degassing or degassed under kinetic (non-equilibrium) conditions, then the δ^{13}C value of the Martian mantle likely reflects accretion from thermally processed undifferentiated (ordinary chondrite-like) and differentiated NC materials. Conversely, if significant degassing occurred via Rayleigh fractionation under equilibrium conditions, the Martian mantle would have a higher δ^{13}C value (−12 to −10 ‰) than observed in Martian meteorites – though still lower than the canonical BSE estimate – implying an additional contribution from ^{13}C-enriched sources from the NC reservoir, such as enstatite chondrite-like materials. While the canonical C isotopic composition of the BSE overlaps with those of enstatite chondrites and ureilites, the late delivery of volatile-rich CC materials during the main phase of Earth's accretion likely biased the BSE's C isotopic composition towards a CC-like signature. However, a lower mean δ^{13}C value of −8.4 ‰ of the MORB mantle, as proposed by recent studies, could mean that Earth's mantle still preserves the signature of ^{13}C-poor, thermally processed NC materials accreted during the early stages of the planet's growth. The observed heterogeneity in mantle C isotopic compositions, similar to that seen in H and N isotopes, could therefore reflect a mixed contribution from both NC and CC materials. This suggests that the δ^{13}C value of the BSE could be lower than the canonical estimate and may align more closely with the proposed value for the MORB mantle.

Data availability

Data are available through Mendeley Data at https://doi.org/10.17632/y3htjsg9rf.2.

CRediT authorship contribution statement

Damanveer S. Grewal: Writing – original draft, Visualization, Validation, Resources, Project administration, Methodology, Investigation, Funding acquisition, Formal analysis, Data curation, Conceptualization. **Sujoy Mukhopadhyay:** Writing – review & editing, Validation, Investiagtion.

Declaration of competing interest

The authors declare that they have no known competing financial interests or personal relationships that could have appeared to influence the work reported in this paper.

Acknowledgements

This study was funded by startup funds from Yale University to D.S. G. We thank three anonymous reviewers for their constructive comments.

Appendix A. Supplementary material

This files contains two supplementary data tables. Table S1 contains the raw meteorite data used to calculate the mean values reported in Table 1, and Table S2 reports the methodology used to collect the data reported in Table S1. Supplementary material to this article can be found online at https://doi.org/10.1016/j.gca.2025.09.014.

References

Abernethy, F.A.J., Verchovsky, A.B., Franchi, I.A., Grady, M.M., 2018. Basaltic volcanism on the angrite parent body: comparison with 4 Vesta. Meteorit. Planet. Sci. 53, 375–393.

Abernethy, F.A.J., Verchovsky, A.B., Starkey, N.A., Anand, M., Franchi, I.A., Grady, M. M., 2013. Stable isotope analysis of carbon and nitrogen in angrites. Meteorit. Planet. Sci. 48, 1590–1606.

Albarède, F., Ballhaus, C., Blichert-Toft, J., Lee, C.-T., Marty, B., Moynier, F., Yin, Q.-Z., 2013. Asteroidal impacts and the origin of terrestrial and lunar volatiles. Icarus 222, 44–52.

Alexander, C.M.O.'D., 2022. An exploration of whether Earth can be built from chondritic components, not bulk chondrites. Geochim. Cosmochim. Acta 318, 428–451.

Alexander, C.M.O.'D., Bowden, R., Fogel, M.L., Howard, K.T., Herd, C.D.K., Nittler, L.R., 2012. The Provenances of Asteroids, and their Contributions to the Volatile inventories of the Terrestrial Planets. Science 337, 721–723.

Alexander, C.M.O.'D., Cody, G.D., De Gregorio, B.T., Nittler, L.R., Stroud, R.M., 2017. The nature, origin and modification of insoluble organic matter in chondrites, the major source of Earth's C and N. Geochemistry 77, 227–256.

Alexander, C.M.O.'D., Bowden, R., Fogel, M.L., Howard, K.T., 2015. Carbonate abundances and isotopic compositions in chondrites. Meteorit. Planet. Sci. 50, 810–833.

Alexander, C.M.O.'D., Fogel, M., Yabuta, H., Cody, G.D., 2007. The origin and evolution of chondrites recorded in the elemental and isotopic compositions of their macromolecular organic matter. Geochim. Cosmochim. Acta 71, 4380–4403.

Alexander, C.M.O'D., Greenwood, R.C., Bowden, R., Gibson, J.M., Howard, K.T., Franchi, I.A., 2018a. A mutli-technique search for the most primitive CO chondrites. Geochim. Cosmochim. Acta 221, 406–420.

Alexander, C.M.O'D., McKeegan, K.D., Altwegg, K., 2018b. Water Reservoirs in Small Planetary Bodies: Meteorites, Asteroids, and Comets. Space Sci. Rev. 214, 36.

Alexander, C.M.O.'D., Russell, S.S., Arden, J.W., Ash, R.D., Grady, M.M., Pillinger, C.T., 1998. The origin of chondritic macromolecular organic matter: a carbon and nitrogen isotope study. Meteorit. Planet. Sci. 33, 603–622.

Aubaud, C., 2022. Carbon stable isotope constraints on CO2 degassing models of ridge, hotspot and arc magmas. Chem. Geol. 605.

Barrat, J.A., Sansjofre, P., Yamaguchi, A., Greenwood, R.C., Gillet, P., 2017. Carbon isotopic variation in ureilites: evidence for an early, volatile-rich Inner Solar System. Earth Planet. Sci. Lett. 478, 143–149.

Barrett, T.J., Bryson, J.F.J., Geraki, K., 2025. The source of hydrogen in earth's building blocks. Icarus.

Brearley A.J., 2006 The action of water. In: Meteorites and the Early Solar System II (eds. D. S. Lauretta and H. Y. McSween Jr.). The University of Arizona Press, Tucson. pp. 587–624.

Breuer, D., Spohn, T., 2003. Early plate tectonics versus single-plate tectonics on Mars: evidence from magnetic field history and crust evolution. J. Geophys. Res. Planets 108.

Broadley, M.W., Bekaert, D.V., Piani, L., Füri, E., Marty, B., 2022. Origin of life-forming volatile elements in the inner Solar System. Nature 611, 245–255.

Budde, G., Burkhardt, C., Kleine, T., 2019. Molybdenum isotopic evidence for the late accretion of outer Solar System material to Earth. Nat. Astron 3, 736–741.

Burkhardt, C., Spitzer, F., Morbidelli, A., Budde, G., Render, J.H., Kruijer, T.S., Kleine, T., 2021. Terrestrial planet formation from lost inner solar system material. Sci. Adv. 7, 7601.

Carr, R.H., Grady, M.M., Wright, I.P., Pillinger, C.T., 1985. Martian atmospheric carbon dioxide and weathering products in SNC meteorites. Nature 314, 248–250.

Cartigny, P., 2005. Stable isotopes and the origin of diamond. Elements 1, 79–84.

Cartigny, P., Harris, J.W., Phillips, D., Girard, M., Javoy, M., 1998. Subduction-related diamonds? — The evidence for a mantle-derived origin from coupled δ13C–δ15N determinations. Chem. Geol. 147, 147–159.

Cartigny, P., Marty, B., 2013. Nitrogen isotopes and mantle geodynamics: the emergence of life and the atmosphere-crust-mantle connection. Elements 9, 359–366.

Clog, M., Lindgren, P., Modestou, S., McDonald, A., Tait, A., Donnelly, T., Mark, D., Lee, M., 2024. Clumped isotope and Δ17O measurements of carbonates in CM carbonaceous chondrites: new insights into parent body thermal and fluid evolution. Geochim. Cosmochim. Acta 369, 1–16.

Cody, G.D., Alexander, C.M.O., Yabuta, H., Kilcoyne, A.L.D., Araki, T., Ade, H., Dera, P., Fogel, M., Militzer, B., Mysen, B.O., 2008. Organic thermometry for chondritic parent bodies. Earth Planet. Sci. Lett. 272, 446–455.

Dalou, C., Hirschmann, M.M., von der Handt, A., Mosenfelder, J., Armstrong, L.S., 2017. Nitrogen and carbon fractionation during core–mantle differentiation at shallow depth. Earth Planet. Sci. Lett. 458, 141–151.

Dasgupta, R., Chi, H., Shimizu, N., Buono, A.S., Walker, D., 2013. Carbon solution and partitioning between metallic and silicate melts in a shallow magma ocean: implications for the origin and distribution of terrestrial carbon. Geochim. Cosmochim. Acta 102, 191–212.

Dasgupta, R., Grewal D.S., 2019. Origin and Early Differentiation of Carbon and Associated Life-Essential Volatile Elements on Earth. In: Deep Carbon: Past to Present (eds. B. Orcutt, I. Daniel, and R. Dasgupta). Cambridge University Press. pp. 4–39.

Dauphas, N., 2017. The isotopic nature of the Earth's accreting material through time. Nature 541, 521–524.

Dauphas, N., Hopp, T., Nesvorný, D., 2024. Bayesian inference on the isotopic building blocks of Mars and Earth. Icarus 408.

Dauphas, N., Pourmand, A., 2011. Hf–W–Th evidence for rapid growth of Mars and its status as a planetary embryo. Nature 473, 489–492.

Deguen, R., Landeau, M., Olson, P., 2014. Turbulent metal-silicate mixing, fragmentation, and equilibration in magma oceans. Earth Planet. Sci. Lett. 391, 274–287.

Deines, P., 2002. The carbon isotope geochemistry of mantle xenoliths. Earth Sci. Rev. 58, 247–278.

Deines, P., Wickman, F.E., 1975. A contribution to the stable carbon isotope geochemistry of iron meteorites. Geochim. Cosmochim. Acta 39, 547–557.

Deines, P., Wickman, F.E., 1973. The isotopic composition of "graphitic" carbon from iron meteorites and some remarks on the troilitic sulfur of iron meteorites. Geochim. Cosmochim. Acta 37, 1295–1319.

Deligny, C., Füri, E., Deloule, E., Peslier, A.H., Faure, F., Marrocchi, Y., 2023. Origin of nitrogen on Mars: first in situ N isotope analyses of martian meteorites. Geochim. Cosmochim. Acta 344, 134–145.

Deloule, E., Albarede, F., Sheppard, S.M.F., 1991. Hydrogen isotope heterogeneities in the mantle from ion probe analysis of amphiboles from ultramafic rocks. Earth Planet Sci. Lett. 105, 543–553.

Dottin III, J.W., Horton, F., Alexander, C.M.O., Shahar, A., Wang, J., Boesenberg, J.S., Bullock, E., Shirey, S.B., 2025. Hydrogen isotopic evidence for a core component in Baffin Island lavas. Sci. Adv. 11, 2917.

Downes, H., Abernethy, F.A.J., Smith, C.L., Ross, A.J., Verchovsky, A.B., Grady, M.M., Jenniskens, P., Shaddad, M.H., 2015. Isotopic composition of carbon and nitrogen in ureilitic fragments of the Almahata Sitta meteorite. Meteorit. Planet. Sci. 50, 255–272.

Fine, G., Stolper, E., 1986. Dissolved carbon dioxide in basaltic glasses: concentrations and speciation. Earth Planet. Sci. Lett. 76, 263–278.

Fine, G., Stolper, E., 1985. The speciation of carbon dioxide in sodium aluminosilicate glasses. Contrib. Miner. Petrol. 91, 105–121.

Foustoukos, D.I., Alexander, D., Cody, G.D., 2021. H and N systematics in thermally altered chondritic insoluble organic matter: an experimental study. Geochim. Cosmochim. Acta 300, 44–64.

Fujiya, W., Hoppe, P., Ushikubo, T., Fukuda, K., Lindgren, P., Lee, M.R., Koike, M., Shirai, K., Sano, Y., 2019. Migration of D-type asteroids from the outer Solar System inferred from carbonate in meteorites. Nat. Astron 3.

Fujiya, W., Kawasaki, N., Nagashima, K., Sakamoto, N., O'D. Alexander, C.M.O.'D., Kita, N.T., Kitajima, K., Abe, Y., Aléon, J., Amari, S., Amelin, Y., Bajo, K., Bizzarro, M., Bouvier, A., Carlson, R.W., Chaussidon, M., Choi, B.-G., Dauphas, N., Davis, A.M., Di Rocco, T., Fukai, R., Gautam, I., Haba, M.K., Hibiya, Y., Hidaka, H., Homma, H., Hoppe, P., Huss, G.R., Ichida, K., Iizuka, T., Ireland, T.R., Ishikawa, A., Itoh, S., Kleine, T., Komatani, S., Krot, A.N., Liu, M.-C., Masuda, Y., McKeegan, K.D., Morita, M., Motomura, K., Moynier, F., Nakai, I., Nguyen, A., Nittler, L., Onose, M., Pack, A., Park, C., Piani, L., Qin, L., Russell, S.S., Schönbächler, M., Tafla, L., Tang, H., Terada, K., Terada, Y., Usui, T., Wada, S., Wadhwa, M., Walker, R.J., Yamashita, K., Yin, Q.-Z., Yokoyama, T., Yoneda, S., Young, E.D., Yui, H., Zhang, A.-C., Nakamura, T., Naraoka, H., Noguchi, T., Okazaki, R., Sakamoto, K., Yabuta, H., Abe, M., Miyazaki, A., Nakato, A., Nishimura, M., Okada, T., Yada, T., Yogata, K., Nakazawa, S., Saiki, T., Tanaka, S., Terui, F., Tsuda, Y., Watanabe, S., Yoshikawa, M., Tachibana, S., Yurimoto, H., 2023. Carbonate record of temporal change in oxygen fugacity and gaseous species in asteroid Ryugu. Nat. Geosci. 16, 675–682.

Gilmour, I., 2003. Structural and isotopic analysis of organic matter in carbonaceous chondrites. Treatise on Geochemistry Elsevier. 269–290.

Glavin, D.P., Alexander, C.M.O.'D., Aponte, J.C., Dworkin, J.P., Elsila, J.E., Yabuta, H., 2018. The origin and evolution of organic matter in carbonaceous chondrites and links to their parent bodies. In Primitive Meteorites and Asteroids Elsevier. 205–271.

Goodrich, C.A., Hartmann, W.K., O'Brien, D.P., Weidenschilling, S.J., Wilson, L., Michel, P., Jutzi, M., 2015. Origin and history of ureilitic material in the solar system: the view from asteroid 2008 TC3 and the Almahata Sitta meteorite. Meteorit. Planet. Sci. 50, 782–809.

Goodrich, C.A., Jones, J.H., Berkley, J.L., 1987. Origin and evolution of the ureilite parent magmas: Multi-stage igneous activity on a large parent body. Geochim. Cosmochim. Acta 51, 2255–2273.

Grady, M.M., Wright, I.P., Pillinger, C.T., 1989. A preliminary investigation into the nature of carbonaceous material in ordinary chondrites. Meteoritics 24, 147–154.

Grady, M.M., Pillinger, C.T., 1986. Carbon isotope relationships in winonaites and forsterite chondrites. Geochim. Cosmochim. Acta 50, 255–263.

Grady, M.M., Swart, P.K., Pillinger, C.T., 1982. The variable carbon isotopic composition of type 3 ordinary chondrites. J. Geophys. Res. Solid Earth 87.

Grady, M.M., Verchovsky, A.B., Wright, I.P., 2004. Magmatic carbon in Martian meteorites: attempts to constrain the carbon cycle on Mars. Int. J. Astrobiol. 3, 117–124.

Grady, M.M., Wright, I.P., Carr, L.P., Pillinger, C.T., 1986. Compositional differences in enstatite chondrites based on carbon and nitrogen stable isotope measurements. Geochim. Cosmochim. Acta 50, 2799–2813.

Grady, M.M., Wright, I.P., Pillinger, C.T., 1997a. A carbon and nitrogen isotope study of Zagami. J. Geophys. Res. Planets 102, 9165–9173.

Grady, M.M., Wright, I.P., Pillinger, C.T., 1997b. Carbon in howardite, eucrite and diogenite basaltic achondrites. Meteorit. Planet. Sci. 32, 863–868.

Grady, M.M., Wright, I.P., Swart, P.K., Pillinger, C.T., 1985. The carbon and nitrogen isotopic composition of ureilites: Implications for their genesis. Geochim. Cosmochim. Acta 49, 903–915.

Grewal, D.S., 2022. Origin of nitrogen isotopic variations in the rocky bodies of the solar system. Astrophys J 937, 123.

Grewal, D.S., Asimow, P.D., 2023. Origin of the superchondritic carbon/nitrogen ratio of the bulk silicate Earth – an outlook from iron meteorites. Geochim. Cosmochim. Acta 344, 146–159.

Grewal, D.S., Bhattacharjee, S., Mardaru, G.-D., Asimow, P.D., 2025a. Tracing the origin of volatiles on Earth using nitrogen isotope ratios in iron meteorites. Geochim. Cosmochim. Acta 388, 34–47.

Grewal, D.S., Bhattacharjee, S., Zhang, B., Nie, N.X., Miyazaki, Y., 2025b. Enrichment of moderately volatile elements in first-generation planetesimals of the inner Solar System. Sci. Adv. 11, 7848.

Grewal, D.S., Dasgupta, R., Aithala, S., 2021a. The effect of carbon concentration on its core-mantle partitioning behavior in inner Solar System rocky bodies. Earth Planet. Sci. Lett. 571, 117090.

Grewal, D.S., Dasgupta, R., Farnell, A., 2020. The speciation of carbon, nitrogen, and water in magma oceans and its effect on volatile partitioning between major reservoirs of the Solar System rocky bodies. Geochim. Cosmochim. Acta 280, 281–301.

Grewal, D.S., Dasgupta, R., Holmes, A.K., Costin, G., Li, Y., Tsuno, K., 2019a. The fate of nitrogen during core-mantle separation on Earth. Geochim. Cosmochim. Acta 251, 87–115.

Grewal, D.S., Dasgupta, R., Hough, T., Farnell, A., 2021b. Rates of protoplanetary accretion and differentiation set nitrogen budget of rocky planets. Nat. Geosci. 14, 369–376.

Grewal, D.S., Dasgupta, R., Marty, B., 2021c. A very early origin of isotopically distinct nitrogen in inner Solar System protoplanets. Nat. Astron 5, 356–364.

Grewal, D.S., Dasgupta, R., Sun, C., Tsuno, K., Costin, G., 2019b. Delivery of carbon, nitrogen, and sulfur to the silicate Earth by a giant impact. Sci. Adv. 5, eaau3669.

Grewal, D.S., Manilal, V., 2025. Implications of Differentiated late Accretion for the Volatile Inventory of the Bulk Silicate Earth. Planet Sci J 6, 13.

Grewal, D.S., Miyazaki, Y., Nie, N.X., 2024a. Contribution of the Moon-forming Impactor to the Volatile Inventory in the Bulk Silicate Earth. Planet Sci J 5, 181.

Grewal, D.S., Nie, N.X., Zhang, B., Izidoro, A., Asimow, P.D., 2024b. Accretion of the earliest inner Solar System planetesimals beyond the water snowline. Nat. Astron 8, 290–297.

Grewal, D.S., Seales, J.D., Dasgupta, R., 2022a. Internal or external magma oceans in the earliest protoplanets – Perspectives from nitrogen and carbon fractionation. Earth Planet. Sci. Lett. 598, 117847.

Grewal, D.S., Sun, T., Aithala, S., Hough, T., Dasgupta, R., Yeung, L.Y., Schauble, E.A., 2022b. Limited nitrogen isotopic fractionation during core-mantle differentiation in rocky protoplanets and planets. Geochim. Cosmochim. Acta 338, 347–364.

Guo W. and Eiler J. M. (2007) Temperatures of aqueous alteration and evidence for methane generation on the parent bodies of the CM chondrites.

Hakim, K., Spaargaren, R., Grewal, D.S., Rohrbach, A., Berndt, J., Dominik, C., Van Westrenen, W., 2019. Mineralogy, structure, and habitability of carbon-enriched rocky exoplanets: a laboratory approach. Astrobiology 19, 867–884.

Halliday, A.N., 2013. The origins of volatiles in the terrestrial planets. Geochim. Cosmochim. Acta 105, 146–171.

Hevey, P.J., Sanders, I.S., 2006. A model for planetesimal meltdown by 26 Al and its implications for meteorite parent bodies. Meteorit. Planet. Sci. 41, 95–106.

Hirschmann, M.M., 2018. Comparative deep Earth volatile cycles: the case for C recycling from exosphere/mantle fractionation of major (H2O, C, N) volatiles and from H2O/Ce, CO2/Ba, and CO2/Nb exosphere ratios. Earth Planet. Sci. Lett. 502, 262–273.

Hirschmann, M.M., 2016. Constraints on the early delivery and fractionation of Earth's major volatiles from C/H, C/N, and C/S ratios. Am. Mineral. 101, 540–553.

Holloway, J.R., Pan, V., Gudmundsson, G., 1992. High-pressure fluid-absent melting experiments in the presence of graphite: oxygen fugacity, ferric/ferrous ratio and dissolved CO2. Eur. J. Mineral. 4, 105–114.

Horita, J., Polyakov, V.B., 2015. Carbon-bearing iron phases and the carbon isotope composition of the deep Earth. Proc. Natl. Acad. Sci. 112, 31–36.

Horton, F., Asimow, P.D., Farley, K.A., Curtice, J., Kurz, M.D., Blusztajn, J., Biasi, J.A., Boyes, X.M., 2023. Highest terrestrial 3He/4He credibly from the core. Nature 623, 90–94.

Huss G.R., Rubin A.E., Grossman J. N., 2006 Thermal Metamorphism in Chondrites. In: Meteorites and the early solar system II (eds. D. S. Lauretta and H. Y. McSween Jr.). University of Arizona Press. pp. 567–586.

Javoy, M., 1995. The integral enstatite chondrite model of the Earth. Geophys. Res. Lett. 22, 2219–2222.

Javoy, M., Pineau, F., 1991. The volatiles record of a "popping" rock from the Mid-Atlantic Ridge at 14°N: chemical and isotopic composition of gas trapped in the vesicles. Earth Planet. Sci. Lett. 107, 598–611.

Javoy, M., Pineau, F., Iiyama, I., 1978. Experimental determination of the isotopic fractionation between gaseous CO2 and carbon dissolved in tholeiitic magma a preliminary study. Contrib. Miner. Petrol. 67, 35–39.

Jull, A.J.T., Eastoe, C.J., Xue, S., Herzog, G.F., 1995. Isotopic composition of carbonates in the SNC meteorites Allan Hills 84001 and Nakhla. Meteoritics 30, 311–318.

Keppler, H., Golabek, G., 2019. Graphite floatation on a magma ocean and the fate of carbon during core formation. Geochem. Perspect. Lett. 11, 12–17.

Kleine, T., Steller, T., Burkhardt, C., Nimmo, F., 2023. An inner solar system origin of volatile elements in Mars. Icarus 397, 115519.

Kleine, T., Touboul, M., Bourdon, B., Nimmo, F., Mezger, K., Palme, H., Jacobsen, S.B., Yin, Q.Z., Halliday, A.N., 2009. Hf-W chronology of the accretion and early evolution of asteroids and terrestrial planets. Geochim. Cosmochim. Acta 73, 5150–5188.

Kruijer, T.S., Burkhardt, C., Budde, G., Kleine, T., 2017. Age of Jupiter inferred from the distinct genetics and formation times of meteorites. Proc. Natl. Acad. Sci. 114, 6712–6716.

Kruijer, T.S., Touboul, M., Fischer-Godde, M., Bermingham, K.R., Walker, R.J., Kleine, T., 2014. Protracted core formation and rapid accretion of protoplanets. Science 344, 1150–1154.

Landeau, M., Deguen, R., Phillips, D., Neufeld, J.A., Lherm, V., Dalziel, S.B., 2021. Metal-silicate mixing by large Earth-forming impacts. Earth Planet. Sci. Lett. 564, 116888.

Lauretta D. S., Connolly H. C., Aebersold J. E., Alexander C. M. O., Ballouz R., Barnes J. J., Bates H. C., Bennett C. A., Blanche L., Blumenfeld E. H., Clemett S. J., Cody G. D., DellaGiustina D. N., Dworkin J. P., Eckley S. A., Foustoukos D. I., Franchi I. A., Glavin D. P., Greenwood R. C., Haenecour P., Hamilton V. E., Hill D. H., Hiroi T., Ishimaru K., Jourdan F., Kaplan H. H., Keller L. P., King A. J., Koefoed P., Kontogiannis M. K., Le L., Macke R. J., McCoy T. J., Milliken R. E., Najorka J., Nguyen A. N., Pajola M., Polit A. T., Righter K., Roper H. L., Russell S. S., Ryan A. J., Sandford S. A., Schofield P. F., Schultz C. D., Seifert L. B., Tachibana S., Thomas-Keprta K. L., Thompson M. S., Tu V., Tusberti F., Wang K., Zega T. J. and Wolner C. W. V. (2024) Asteroid (101955) Bennu in the laboratory: Properties of the sample collected by OSIRIS-REx. *Meteorit Planet Sci*.

Lawrence, W.M., Blake G.A., Eiler J., 2025. Carbon and oxygen isotope evidence for a protoplanetary disk origin of organic solids in meteorites. In: Proceedings of the National Academy of Sciences **122**.

Lee H., Moussallam Y., Aubaud C., Iacono–Marziano G., Hammond K., Ebel D., 2024. Carbon isotope fractionation between CO2 and carbon in silicate melts at high temperature. Geochim Cosmochim Acta 380, 208–219.

Li, Y., Dasgupta, R., Tsuno, K., 2017. Carbon contents in reduced basalts at graphite saturation: Implications for the degassing of Mars, Mercury, and the Moon. J. Geophys. Res. Planets 122, 1300–1320.

Li, Y., Wiedenbeck, M., Monteleone, B., Dasgupta, R., Costin, G., Gao, Z., Lu, W., 2023. Nitrogen and carbon fractionation in planetary magma oceans and origin of the superchondritic C/N ratio in the bulk silicate Earth. Earth Planet. Sci. Lett. 605, 118032.

Lichtenberg, T., Drążkowska, J., Schönbächler, M., Golabek, G.J., Hands, T.O., 2021. Bifurcation of planetary building blocks during Solar System formation. Science 371, 365–370.

Lichtenberg, T., Golabek, G.J., Burn, R., Meyer, M.R., Alibert, Y., Gerya, T.V., Mordasini, C., 2019. A water budget dichotomy of rocky protoplanets from 26Al-heating. Nat. Astron 3, 307–313.

Loewen, M.W., Graham, D.W., Bindeman, I.N., Lupton, J.E., Garcia, M.O., 2019. Hydrogen isotopes in high 3 He/ 4 He submarine basalts: Primordial vs. recycled water and the veil of mantle enrichment. Earth Planet. Sci. Lett. 508, 62–73.

Marrocchi, Y., Avice, G., Barrat, J.-A., 2021. The Tarda meteorite: a window into the formation of D-type asteroids. Astrophys J Lett 913, L9.

Martins, R., Kuthning, S., Coles, B.J., Kreissig, K., Rehkämper, M., 2023. Nucleosynthetic isotope anomalies of zinc in meteorites constrain the origin of Earth's volatiles. Science 379, 369–372.

Marty, B., 2012. The origins and concentrations of water, carbon, nitrogen and noble gases on Earth. Earth Planet. Sci. Lett. 313–314, 56–66.

Marty, B., Alexander, C.M.O.D., Raymond, S.N., 2013. Primordial origins of earth's carbon. Rev. Mineral. Geochem. 75, 149–181.

Marty B., Almayrac M., Barry P. H., Bekaert D. V, Broadley M. W., Byrne D. J., Ballentine C.J., Caracausi A., 2020. An evaluation of the C/N ratio of the mantle from natural CO2-rich gas analysis: Geochemical and cosmochemical implications. Earth Planet Sci Lett 551, 116574.

Mathew, K.J., Marti, K., 2001. Early evolution of Martian volatiles: Nitrogen and noble gas components in ALH84001 and Chassigny. J. Geophys. Res. Planets 106, 1401–1422.

Mathew, K.J., Marty, B., Marti, K., Zimmermann, L., 2003. Volatiles (nitrogen, noble gases) in recently discovered SNC meteorites, extinct radioactivities and evolution. Earth Planet. Sci. Lett.

Mattey, D.P., 1991. Carbon dioxide solubility and carbon isotope fractionation in basaltic melt. Geochim. Cosmochim. Acta 55, 3467–3473.

Mattey, D.P., Taylor, W.R., Green, D.H., Pillinger, C.T., 1990. Carbon isotopic fractionation between CO2 vapour, silicate and carbonate melts: an experimental study to 30 kbar. Contrib. Miner. Petrol. 104, 492–505.

McCubbin, F.M., Hauri, E.H., Elardo, S.M., Vander, Kaaden, K.E., Wang, J., Shearer, C.K., 2012. Hydrous melting of the martian mantle produced both depleted and enriched shergottites. Geology 40, 683–686.

Mizutani, S., Satish-Kumar, M., Yoshino, T., 2014. Experimental determination of carbon isotope fractionation between graphite and carbonated silicate melt under upper mantle conditions. Earth Planet. Sci. Lett. 392, 86–93.

Mohapatra, R.K., Murty, S.V.S., 2003. Precursors of Mars: Constraints from nitrogen and oxygen isotopic compositions of martian meteorites. Meteorit. Planet. Sci. 38, 225–241.

Monnereau, M., Toplis, M.J., Baratoux, D., Guignard, J., 2013. Thermal history of the H-chondrite parent body: implications for metamorphic grade and accretionary time-scales. Geochim. Cosmochim. Acta 119, 302–321.

Morbidelli, A., Kleine, T., Nimmo, F., 2025. Did the terrestrial planets of the solar system form by pebble accretion? Earth Planet Sci Lett 650.

Moussallam, Y., 2025. Carbon isotopes in magmatic systems: measurements, interpretations, and the carbon isotopic signature of the Earth's Mantle. Geosciences (Basel) 15, 266.

Moussallam, Y., Koga, K.T., Rose-Koga, E.F., Aubaud, C., Lee, H.J., Georgeais, G., 2025a. The carbon isotopic signature of the upper mantle is heterogeneous. Commun. Earth Environ. 6, 6.

Moussallam Y., Rose-Koga E. F., Aubaud C., Georgeais G., Cartigny P., Koga K. T., Devidal J.-L., Michael P. J., Shimizu K., Saal A.E., 2025b. Enigmatic carbon isotopic variability in the oceanic upper mantle. Proc. Natl. Acad. Sci. 122.

Moussallam Y., Rose-Koga E. F., Fischer T. P., Georgeais G., Lee H. J., Birnbaum J., Pfeffer M. A., Barnie T., Regis E., 2024. Kinetic Isotopic Degassing of CO2 During the 2021 Fagradalsfjall Eruption and the δ13C Signature of the Icelandic Mantle. Geochem. Geophys. Geosyst. 25.

Mundl-Petermeier, A., Walker, R.J., Fischer, R.A., Lekic, V., Jackson, M.G., Kurz, M.D., 2020. Anomalous 182W in high 3He/4He ocean island basalts: Fingerprints of Earth's core? Geochim. Cosmochim. Acta 271, 194–211.

Naraoka, H., Takano, Y., Dworkin, J.P., Oba, Y., Hamase, K., Furusho, A., Ogawa, N.O., Hashiguchi, M., Fukushima, K., Aoki, D., Schmitt-Kopplin, P., Aponte, J.C., Parker, E.T., Glavin, D.P., McLain, H.L., Elsila, J.E., Graham, H.V., Eiler, J.M., Orthous-Daunay, F.-R., Wolters, C., Isa, J., Vuitton, V., Thissen, R., Sakai, S., Yoshimura, T., Koga, T., Ohkouchi, N., Chikaraishi, Y., Sugahara, H., Mita, H., Furukawa, Y., Hertkorn, N., Ruf, A., Yurimoto, H., Nakamura, T., Noguchi, T., Okazaki, R., Yabuta, H., Sakamoto, K., Tachibana, S., Connolly, H.C., Lauretta, D.S., Abe, M., Yada, T., Nishimura, M., Yogata, K., Nakato, A., Yoshitake, M., Suzuki, A., Miyazaki, A., Furuya, S., Hatakeda, K., Soejima, H., Hitomi, Y., Kumagai, K., Usui, T., Hayashi, T., Yamamoto, D., Fukai, R., Kitazato, K., Sugita, S., Namiki, N., Arakawa, M., Ikeda, H., Ishiguro, M., Hirata Naru, Wada, K., Ishihara, Y., Noguchi, R., Morota, T., Sakatani, N., Matsumoto, K., Senshu, H., Honda, R., Tatsumi, E., Yokota, Y., Honda, C., Michikami, T., Matsuoka, M., Miura, A., Noda, H., Yamada, T., Yoshihara, K., Kawahara, K., Ozaki, M., Iijima, Y., Yano, H., Hayakawa, M., Iwata, T., Tsukizaki, R., Sawada, H., Hosoda, S., Ogawa, K., Okamoto, C., Hirata Naoyuki, Shirai, K., Shimaki, Y., Yamada, M., Okada, T., Yamamoto, Y., Takeuchi, H., Fujii, A., Takei, Y., Yoshikawa, K., Mimasu, Y., Ono, G., Ogawa, N., Kikuchi, S., Nakazawa, S., Terui, F., Tanaka, S., Saiki, T., Yoshikawa, M., Watanabe, S., Tsuda, Y., 2023. Soluble organic molecules in samples of the carbonaceous asteroid (162173) Ryugu. Science 379, 27.

Nicklas R. W., Day J. M. D., Vaci Z., Udry A., Liu Y. and Tait K. T. (2021) Uniform oxygen fugacity of shergottite mantle sources and an oxidized martian lithosphere. Earth Planet Sci Lett 564.

Nimmo, F., Kleine, T., Morbidelli, A., Nesvorny, D., 2024. Mechanisms and timing of carbonaceous chondrite delivery to the Earth. Earth Planet. Sci. Lett. 648, 119112.

Ordonez C.G., Jiang Z., Greenwood, J.P., Sakamoto N., 2024. Water in Almahata Sitta Enstatite Chondrite Pyroxene. In 55th Lunar and Planetary Science Conference.

Paquet, M., Sossi, P.A., Moynier, F., 2023. Origin and abundances of volatiles on Mars from the zinc isotopic composition of Martian meteorites. Earth Planet. Sci. Lett. 611, 118126.

Pearson, V.K., Sephton, M.A., Franchi, I.A., Gibson, J.M., Gilmour, I., 2006. Carbon and nitrogen in carbonaceous chondrites: elemental abundances and stable isotopic compisitions. Meteorit. Planet. Sci. 41, 1899–1918.

Péron, S., Mukhopadhyay, S., Kurz, M.D., Graham, D.W., 2021. Deep-mantle krypton reveals Earth's early accretion of carbonaceous matter. Nature 600, 462–467.

Peslier, A.H., Hervig, R., Yang, S., Humayun, M., Barnes, J.J., Irving, A.J., Brandon, A.D., 2019. Determination of the water content and D/H ratio of the martian mantle by unraveling degassing and crystallization effects in nakhlites. Geochim. Cosmochim. Acta 266, 382–415.

Peterson, L.D., Newcombe, M.E., Alexander, C.M.O., Wang, J., Klein, F., Bekaert, D.V., Nielsen, S.G., 2023a. The H content of aubrites: an evaluation of bulk versus in situ methods for quantifying water in meteorites. Earth Planet. Sci. Lett. 620, 118341.

Peterson, L.D., Newcombe, M.E., Alexander, C.M.O., Wang, J., Sarafian, A.R., Bischoff, A., Nielsen, S.G., 2023b. The H2O content of the ureilite parent body. Geochim. Cosmochim. Acta 340, 141–157.

Piani, L., Marrocchi, Y., Rigaudier, T., Vacher, L.G., Thomassin, D., Marty, B., 2020. Earth's water may have been inherited from material similar to enstatite chondrite meteorites. Science 369, 1110–1113.

Pineau, F., Shilobreeva, S., Hekinian, R., Bideau, D., Javoy, M., 2004. Deep-sea explosive activity on the Mid-Atlantic Ridge near 34°50′N: a stable isotope (C, H, O) study. Chem. Geol. 211, 159–175.

Righter, K., Sutton, S.R., Danielson, L., Pando, K., Newville, M., 2016. Redox variations in the inner solar system with new constraints from vanadium XANES in spinels. Am. Mineral. 101, 1928–1942.

Rubie, D.C., Frost, D.J., Mann, U., Asahara, Y., Nimmo, F., Tsuno, K., Kegler, P., Holzheid, A., Palme, H., 2011. Heterogeneous accretion, composition and core-mantle differentiation of the Earth. Earth Planet. Sci. Lett. 301, 31–42.

Russell S.S., Arden J.W., Franchi I.A., Pillinger C.T., 1993. A carbon and nitrogen isotope study of carbonaceous vein material in ureilite meteorites. In: 24th Lunar and Planetary Science Conference.

Sahijpal, S., Soni, P., Gupta, G., 2007. Numerical simulations of the differentiation of accreting planetesimals with 26Al and 60Fe as the heat sources. Meteorit. Planet. Sci. 42, 1529–1548.

Sakuraba, H., Kurokawa, H., Genda, H., Ohta, K., 2021. Numerous chondritic impactors and oxidized magma ocean set Earth's volatile depletion. Sci. Rep. 11, 20894.

Satish-Kumar, M., So, H., Yoshino, T., Kato, M., Hiroi, Y., 2011. Experimental determination of carbon isotope fractionation between iron carbide melt and carbon: 12C-enriched carbon in the Earth's core? Earth Planet. Sci. Lett. 310, 340–348.

Savage, P.S., Moynier, F., Boyet, M., 2022. Zinc isotope anomalies in primitive meteorites identify the outer solar system as an important source of Earth's volatile inventory. Icarus 386, 115172.

Schlichting, H.E., Mukhopadhyay, S., 2018. Atmosphere impact losses. Space Sci. Rev. 214, 34.

Scott, E.R.D., Brearley, A.J., Keil, K., Grady, M.M., Pillinger, C.T., Clayton, R.N., 1987. Nature and origin of C-rich ordinary chondrites and chondritic clasts. In: Lunar and Planetary Science Conference, 18th, Houston, TX.

Schönbächler, M., Carlson, R.W., Horan, M.F., Mock, T.D., Hauri, E.H., 2010. Heterogeneous accretion and the moderately volatile element budget of earth. Science 328, 884–887.

Sephton, M.A., Pillinger, C.T., Gilmour, I., 2000. Aromatic moieties in meteoritic macromolecular materials: analyses by hydrous pyrolysis and δ13C of individual compounds. Geochim. Cosmochim. Acta 64, 321–328.

Sephton, M.A., Verchovsky, A.B., Bland, P.A., Gilmour, I., Grady, M.M., Wright, I.P., 2003. Investigating the variations in carbon and nitrogen isotopes in carbonaceous chondrites. Geochim. Cosmochim. Acta 67, 2093–2108.

Sleep, N.H., 1994. Martian plate tectonics. J. Geophys. Res. Planets 99, 5639–5655.

Smith C. L., Franchi I. A., Wright I. P., Grady M. M. and Pillinger C.T., 2001. New Data on Carbon Isotopic Compositions of Some Ureilites. In 32nd Lunar and Planetary Science Conference.

Stanley, B.D., Hirschmann, M.M., Withers, A.C., 2011. CO2 solubility in Martian basalts and Martian atmospheric evolution. Geochim. Cosmochim. Acta 75, 5987–6003.

Stanley, B.D., Schaub, D.R., Hirschmann, M.M., 2012. CO2 solubility in primitive martian basalts similar to Yamato 980459, the effect of composition on CO2 solubility of basalts, and the evolution of the martian atmosphere. Am. Mineral. 97, 1841–1848.

Steele, A., McCubbin, F.M., Fries, M., Kater, L., Boctor, N.Z., Fogel, M.L., Conrad, P.G., Glamoclija, M., Spencer, M., Morrow, A.L., Hammond, M.R., Zare, R.N., Vicenzi, E. P., Siljeström, S., Bowden, R., Herd, C.D.K., Mysen, B.O., Shirey, S.B., Amundsen, H. E.F., Treiman, A.H., Bullock, E.S., Jull, A.J.T., 2012. A reduced organic carbon component in martian basalts. Science 337, 212–215.

Steenstra, E.S., Dankers, D., Berndt, J., Klemme, S., Matveev, S., van Westrenen, W., 2019. Significant depletion of volatile elements in the mantle of asteroid Vesta due to core formation. Icarus 317, 669–681.

Steller, T., Burkhardt, C., Yang, C., Kleine, T., 2022. Nucleosynthetic zinc isotope anomalies reveal a dual origin of terrestrial volatiles. Icarus 386, 115171.

Storz, J., Ludwig, T., Bischoff, A., Schwarz, W.H., Trieloff, M., 2021. Graphite in ureilites, enstatite chondrites, and unique clasts in ordinary chondrites – Insights from the carbon-isotope composition. Geochim. Cosmochim. Acta 307, 86–104.

Suer T.-A., Jackson C., Grewal D. S., Dalou C. and Lichtenberg, T., 2023. The distribution of volatile elements during rocky planet formation. Front Earth Sci (Lausanne) 11.

Sugiura, N., Fujiya, W., 2014. Correlated accretion ages and ε 54 Cr of meteorite parent bodies and the evolution of the solar nebula. Meteorit. Planet. Sci. 49, 772–787.

Tagawa, S., Sakamoto, N., Hirose, K., Yokoo, S., Hernlund, J., Ohishi, Y., Yurimoto, H., 2021. Experimental evidence for hydrogen incorporation into Earth's core. Nat. Commun. 12, 2588.

Thomassin, D., Piani, L., Villeneuve, J., Caumon, M. C., Bouden, N., Marrocchi, Y., 2023. The high-temperature origin of hydrogen in enstatite chondrite chondrules and implications for the origin of terrestrial water. Earth Planet Sci. Lett. **616**.

Tsuno, K., Grewal, D.S., Dasgupta, R., 2018. Core-mantle fractionation of carbon in Earth and Mars: the effects of sulfur. Geochim. Cosmochim. Acta 238, 477–495.

Tsuno, K., Grewal, D.S., Xu, V., Leinbach, L., Leinenweber, K., Wittmann, A., Shim, S., 2024. The Effect of Nitrogen on the Dihedral Angle Between Fe—Ni Melt and Ringwoodite: implications for the Nitrogen Deficit in the Bulk Silicate Earth. Geophys Res Lett 51.

Tucker, J.M., Mukhopadhyay, S., 2014. Evidence for multiple magma ocean outgassing and atmospheric loss episodes from mantle noble gases. Earth Planet. Sci. Lett. 393, 254–265.

Tucker, J.M., Mukhopadhyay, S., Gonnermann, H.M., 2018. Reconstructing mantle carbon and noble gas contents from degassed mid-ocean ridge basalts. Earth Planet. Sci. Lett. 496, 108–119.

Usui, T., Alexander, C.M.O.D., Wang, J., Simon, J.I., Jones, J.H., 2012. Origin of water and mantle-crust interactions on Mars inferred from hydrogen isotopes and volatile element abundances of olivine-hosted melt inclusions of primitive shergottites. Earth Planet. Sci. Lett. 357–358, 119–129.

Vacher, L.G., Piani, L., Rigaudier, T., Thomassin, D., Florin, G., Piralla, M., Marrocchi, Y., 2020. Hydrogen in chondrites: influence of parent body alteration and atmospheric contamination on primordial components. Geochim. Cosmochim. Acta 281, 53–66.

Vacher, L.G., Piralla, M., Gounelle, M., Bizzarro, M., Marrocchi, Y., 2019a. Thermal evolution of hydrated asteroids inferred from oxygen isotopes. Astrophys J 882, L20.

Vacher, L.G., Truche, L., Faure, F., Tissandier, L., Mosser-Ruck, R., Marrocchi, Y., 2019b. Deciphering the conditions of tochilinite and cronstedtite formation in CM chondrites from low temperature hydrothermal experiments. Meteorit. Planet. Sci. 54, 1870–1889.

Verdier-Paoletti, M.J., Marrocchi, Y., Vacher, L.G., Gattacceca, J., Gurenko, A., Sonzogni, C., Gounelle, M., 2019. Testing the genetic relationship between fluid alteration and brecciation in CM chondrites. Meteorit. Planet. Sci. 54, 1692–1709.

Wasson, J.T., 1972. Formation of ordinary chondrites. Rev. Geophys. 10, 711–759.

Weidenschilling, S.J., 2019. Accretion of the asteroids: Implications for their thermal evolution. Meteorit. Planet. Sci. 54, 1115–1132.

Wright, I.P., Grady, M.M., Pillinger, C.T., 1990. The evolution of atmospheric CO 2 on Mars: the perspective from carbon isotope measurements. J. Geophys. Res. Solid Earth 95, 14789–14794.

Wright, I.P., Grady, M.M., Pillinger, C.T., 1992. Chassigny and the nakhlites: Carbon-bearing components and their relationship to martian environmental conditions. Geochim. Cosmochim. Acta 56, 817–826.

Yesiltas, M., Young, J., Glotch, T.D., 2021. Thermal metamorphic history of Antarctic CV3 and CO3 chondrites inferred from the first- and second-order Raman peaks of polyaromatic organic carbon. Am. Mineral. 106, 506–517.

Yokoyama, T., Nagashima, K., Nakai, I., Young, E.D., Abe, Y., Aléon, J., Alexander, C.M. O., Amari, S., Amelin, Y., Bajo, K., Bizzarro, M., Bouvier, A., Carlson, R.W., Chaussidon, M., Choi, B.-G., Dauphas, N., Davis, A.M., Di Rocco, T., Fujiya, W., Fukai, R., Gautam, I., Haba, M.K., Hibiya, Y., Hidaka, H., Homma, H., Hoppe, P., Huss, G.R., Ichida, K., Iizuka, T., Ireland, T.R., Ishikawa, A., Ito, M., Itoh, S., Kawasaki, N., Kita, N.T., Kitajima, K., Kleine, T., Komatani, S., Krot, A.N., Liu, M.-C., Masuda, Y., McKeegan, K.D., Morita, M., Motomura, K., Moynier, F., Nguyen, A., Nittler, L., Onose, M., Pack, A., Park, C., Piani, L., Qin, L., Russell, S.S., Sakamoto, N., Schönbächler, M., Tafla, L., Tang, H., Terada, K., Terada, Y., Usui, T., Wada, S., Wadhwa, M., Walker, R.J., Yamashita, K., Yin, Q.-Z., Yoneda, S., Yui, H., Zhang, A.-C., Connolly, H.C., Lauretta, D.S., Nakamura, T., Naraoka, H., Noguchi, T., Okazaki, R., Sakamoto, K., Yabuta, H., Abe, M., Arakawa, M., Fujii, A., Hayakawa, M., Naoyuki, H., Naru, H., Honda, R., Honda, C., Hosoda, S., Iijima, Y., Ikeda, H., Ishiguro, M., Ishihara, Y., Iwata, T., Kawahara, K., Kikuchi, S., Kitazato, K., Matsumoto, K., Matsuoka, M., Michikami, T., Mimasu, Y., Miura, A., Morota, T., Nakazawa, S., Namiki, N., Noda, H., Noguchi, R., Ogawa, N., Ogawa, K., Okada, T., Okamoto, C., Ono, G., Ozaki, M., Saiki, T., Sakatani, N., Sawada, H., Senshu, H., Shimaki, Y., Shirai, K., Sugita, S., Takei, Y., Takeuchi, H., Tanaka, S., Tatsumi, E., Terui, F., Tsuda, Y., Tsukizaki, R., Wada, K., Watanabe, S., Yamada, M., Yamada, T., Yamamoto, Y., Yano, H., Yokota, Y., Yoshihara, K., Yoshikawa, M., Yoshikawa, K., Furuya, S., Hatakeda, K., Hayashi, T., Hitomi, Y., Kumagai, K., Miyazaki, A., Nakato, A., Nishimura, M., Soejima, H., Suzuki, A., Yada, T., Yamamoto, D., Yogata, K., Yoshitake, M., Tachibana, S., Yurimoto, H., 2023. Samples returned from the asteroid Ryugu are similar to Ivuna-type carbonaceous meteorites. Science 379.

Yoshioka, T., McCammon, C., Shcheka, S., Keppler, H., 2015. The speciation of carbon monoxide in silicate melts and glasses. Am. Mineral. 100, 1641–1644.

Yoshioka, T., Nakashima, D., Nakamura, T., Shcheka, S., Keppler, H., 2019. Carbon solubility in silicate melts in equilibrium with a CO-CO2 gas phase and graphite. Geochim. Cosmochim. Acta 259, 129–143.

Yoshizaki, T., McDonough, W.F., 2020. The composition of Mars. Geochim. Cosmochim. Acta 273, 137–162.